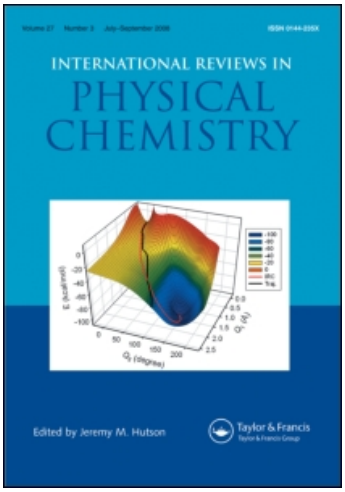

International Reviews in Physical Chemistry
Publication details, including instructions for authors and subscription information:
http://www.informaworld.com/smpp/title~content=t713724383

The chemistry of meteoric metals in the Earth's upper atmosphere

John M. C. Plane[a]
[a] Rosenstiel School of Marine and Atmospheric Science, University of Miami, Miami, Florida, USA

To cite this Article Plane, John M. C.(1991) 'The chemistry of meteoric metals in the Earth's upper atmosphere', International Reviews in Physical Chemistry, 10: 1, 55 — 106
To link to this Article: DOI: 10.1080/01442359109353254
URL: http://dx.doi.org/10.1080/01442359109353254

INTERNATIONAL REVIEWS IN PHYSICAL CHEMISTRY, 1991, VOL. 10, NO. 1, 55–106

The chemistry of meteoric metals in the Earth's upper atmosphere

by JOHN M. C. PLANE
Rosenstiel School of Marine and Atmospheric Science, University of Miami,
4600 Rickenbacker Causeway, Miami, Florida 33149, U.S.A.

The presence of thin layers of free metal atoms at around 90 km in the upper atmosphere has been known for about fifty years. Layers of the alkali metals Na, K and Li, as well as Ca and Fe, have been observed. This discovery has posed two important questions. First, what is the source of the metals: interplanetary or terrestrial? Secondly, what is the nature of the chemistry that causes reactive metals such as sodium to exist in their atomic form in the atmosphere? The first part of this review covers the techniques that have been developed to observe the metal layers, including ground-, rocket- and space-based photometers, and in particular metal lidars. The many curious phenomena that have been observed are then described, such as the small scale-heights of the layers, the quite different seasonal variations of the three alkali metals, the large depletions of Ca and Fe relative to Na, and the dramatic appearance of sporadic Na layers. The second part of the review describes the recent advances that have been made in laboratory kinetic studies of metal reactions of atmospheric interest. A number of specialized techniques for making low-temperature measurements are compared, and a compilation of recommended rate coefficients is given. The history of modelling of the chemistry of metals in the mesosphere is then reviewed, and the evidence that their major source is meteoric ablation is presented. A current model of sodium is then described and evaluated with sensitivity tests. This section ends by discussing the possible impact of these meteoric metals on the chlorine-catalysed removal of ozone in the stratosphere. The final part of the review summarizes the active current state of the field and identifies some of its future directions.

1. Introduction

The input of meteoric material into the Earth's atmosphere is thought to be about 44 tonnes per day (Hughes 1978). Most of this material, which ranges in size from cosmic dust to the large rocks that are able to reach the Earth's surface as meteorites, ablates at altitudes between 80 and 90 km. This happens because below 90 km the atmospheric pressure starts to become significant (greater than 1 mTorr = 0·133 Pa), and the relative meteoroid velocity, which averages about 15 km s^{-1} (Hunten *et al.* 1980), is large enough to cause severe frictional heating of the material. The result of meteoric ablation is that a large flux of metallic vapour is continuously entering the Earth's atmosphere. The major metallic constituents of meteorites are by weight (Mason 1971): Na 0·6%, Ca 1·0%, Ni 1·5%, Al 1·7%, Fe 11·5% and Mg 12·5%. The subsequent chemistry of these metals is the subject of this review.

A full understanding of this chemistry is important for a number of reasons. Firstly, meteoric metals have very unusual atmospheric chemistries, and this makes them inherently worth studying. Secondly, the free metal atoms, which are relatively easy to view with ground-based instruments, appear to be excellent tracers of the dynamical processes that govern this part of the atmosphere, such as tidal forces and gravity waves. Thirdly, the downward flux of these metals into the lower atmosphere may have a significant impact on the chlorine-catalysed removal of ozone in the stratosphere.

0144–235X/91 $3·00

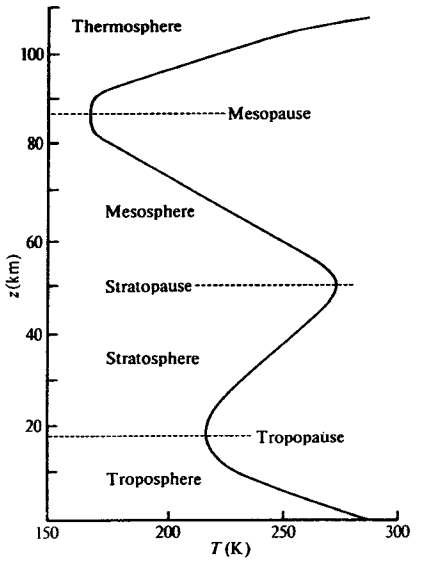

Figure 1. A vertical profile of temperature for the Earth's atmosphere. The curve shown represents the mean structure for latitude 40°N during June. (Reproduced from Wayne (1985).)

The process of meteoric ablation occurs in the mesosphere, the part of the Earth's atmosphere between about 60 and 90 km (see figure 1). The mesosphere represents the boundary between the lower neutral stratosphere and the ionosphere, where species exist predominantly as ions (Wayne 1985). Although until recently the mesosphere had received little attention compared with the other regions of the atmosphere, its importance as a region of energetic coupling between the neutral and ionic regions of the atmosphere is now recognized and is being very actively studied. To a physical chemist, the chemistry of the mesosphere is of great interest because of the extremes of temperature, pressure and solar insolation characterizing the region. For instance, the mesopause is the coldest part of the Earth's atmosphere. In summer, when temperatures are in fact colder than in winter owing to an adiabatic expansion of the mesosphere as the stratosphere becomes warmer, temperatures have been measured down to an extreme of about 100 K in the polar mesopause (Philbrick *et al.* 1984), although summer polar temperatures of 140 K are more normal (CIRA 1972). In the winter, the mesopause warms to 200–220 K (CIRA 1972), representing a nearly twofold increase in temperature. As we shall see below, although reactions cannot possess activation energies larger than about 20 kJ mol^{-1} in order for their rates to be at all significant at these low temperatures, such a large relative temperature change can cause important seasonal variations in the chemistry. The atmospheric pressure varies from about 10 mTorr at 80 km to less than 1 mTorr at the upper boundary of the mesosphere. Thus all termolecular reactions are essentially at their low-pressure limits. Above 100 km, molecular diffusion becomes a more important mode of molecular transport than turbulent or eddy diffusion. Lastly, the solar insolation penetrating through the mesosphere is only attenuated at wavelengths less than 190 nm (Shimazaki 1985). This means that photochemistry requiring photon energies in excess of 5 eV occurs in this region, producing ions and neutral species that are often in highly excited electronic and vibrational states (McEwan and Phillips 1975, Wayne 1985).

Full understanding of a geophysical phenomenon is usually achieved by a combination of observation, laboratory investigation and modelling. In the case of atmospheric chemistry, these three elements are indispensable. Field observations first identify a phenomenon that is inherently interesting or has important implications (e.g. the stratospheric ozone layer) requiring further study and understanding. Laboratory measurements of pertinent chemical parameters such as reaction rate coefficients and photolysis cross-sections are required as input into a model of the phenomenon, whose output can then be tested against further observations in the field. Sensitivity tests indicate where important uncertainties exist in the model. This information is required for planning future laboratory investigations. Once a reasonable confidence level in the predictive capability of the model has been achieved, the model can also be used to determine the most effective strategies for further field observations. These in turn provide a more rigorous test of the model.

The study of the chemistry of meteoric metals in the Earth's upper atmosphere illustrates very well this close relationship between observation, laboratory investigation and modelling. This review has thus been divided into three sections under these headings, which follow this introduction. Section 2 discusses the history of observations of metals in the mesosphere, and identifies the remarkable features of their atmospheric behaviour. Many of the most puzzling observations are very recent and have yet to be explained satisfactorily. Section 3 describes the specialized laboratory techniques that have been developed in the last few years for studying the reaction kinetics and photochemistry of metallic species at the low temperatures characteristic of the mesosphere. The results of these laboratory studies are then reviewed. In section 4, the history of modelling the chemistry of metals in the mesosphere is discussed. A current model is then presented, and a sensitivity analysis is used to identify uncertainties in the chemistry which require laboratory investigation. Models of the impact of metals on the chemistry of stratospheric ozone are also described. The review then concludes with a discussion of future research directions in section 5.

2. Observations of metals in the mesosphere

The first observation of a yellow radiation at 589 nm in the nightglow spectrum was reported by Slipher (1929). This radiation turned out to originate from sodium ($Na(3\,^2P_J - 3\,^2S_{1/2})$) and to be located within the Earth's atmosphere (Bernard 1938a, b, Cabannes *et al.* 1938, Dejardin 1938). Since then, a number of techniques have been developed to study the origin and behaviour of several metals, which exist as free metal atoms in layers centred close to 90 km in the mesosphere. Section 2.1 describes these techniques and lists the types of observations that have been made with them. Section 2.2 then discusses the important features of each of the metals that have so far been observed, stressing their comparative atmospheric behaviour.

2.1. *Techniques for observing atmospheric metals*

2.1.1. *Photometry*

The first quantitative observations of metal atoms were made in the 1950s using ground-based photometers that measured the resonance fluorescence from spectroscopic transitions of the metal atoms, excited by solar radiation. Emission lines from Na, K and Ca^+ were observed during the first two decades of photometric measurements (Hunten 1967), and the first twilight emission from Fe was reported

more recently (Broadfoot and Johanson 1976). The successful observation of emissions from these metals reflects their extremely large resonant scattering cross-sections, since their concentrations relative to the general atmosphere are less than 0·1 parts per billion. Photometers are generally pointed to near zenith during twilight, when the geometrical shadow height of the Earth is close to mesospheric altitudes. This procedure avoids a large signal of Rayleigh-scattered sunlight from the denser lower atmosphere, and the variation of the emission signal as the shadow height passes up through the metal layer provides information on the vertical profile of the layer. The techniques for evaluating the atomic contents and height distributions of the neutral atoms from observation of the twilight glow are well established from the pioneering work in the 1950s of Hunten (1956) and Blamont *et al.* (1958), who elaborated on radiative-transfer theories in order to deduce the metal-atom density profile from the observed integrated line intensity. This work is reviewed by Hunten (1967). Figure 2 illustrates profiles of Na and K obtained from twilight emission measurements. Note the typical narrow layers of the metal atoms at about 90 km.

The emission measurements were extended to the dayglow by using a Zeeman photometer (Blamont *et al.* 1958) and a high-resolution Fabry–Perot spectrometer (McNutt and Mack 1963). Photometers have also been flown on rockets to measure the dayglow (Hunten and Wallace 1967, Donahue and Meier 1967). The daytime Na layer has in addition been observed via the absorption of solar D lines (Neo and Shepherd 1964, Burnett *et al.* 1972).

The D-line emission of Na at 589 nm, which forms part of the nightglow, is generated by a chemiluminescent reaction (Section 4.1), not by resonantly scattered

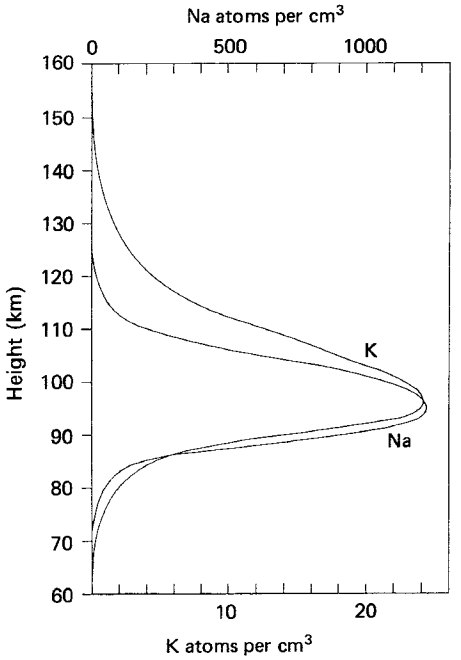

Figure 2. The vertical distribution of potassium and sodium atoms over Saskatoon, 4 April 1962, measured by photometry of the twilight emission. (Reproduced from Sullivan and Hunten (1964).)

sunlight. Thus observation of the nightglow alone does not yield information on the atomic-Na density profile. The Na nightglow is about 30 times weaker than the twilight or dayglow emission. The ground-based measurements reviewed by Kvifte (1973) range between 50 and 200 R (1 R ≡ 1 Rayleigh = 10^6 photons $cm^{-2} s^{-1}$). The nightglow has also been measured by a rocket-borne photometer (Greer and Best 1967) and a photometer placed on a limb-scanning satellite (Newman 1988).

2.1.2. *Lidar*

The discovery of tunable laser sources in the visible allowed direct measurements of the atomic-metal density in the mesosphere by the laser-radar or lidar technique. This was first employed to study atomic Na (Bowman *et al.* 1969, Sandford and Gibson 1970). In this technique, a pulsed dye-laser beam, tuned to a strongly allowed spectroscopic transition of the metal atom of interest, is transmitted upwards through the atmosphere. The laser pulse is Mie- and Rayleigh-scattered, particularly in the lower part of the atmosphere, where there are aerosol layers and the atmospheric pressure is greater. In the mesosphere, the pulse is scattered resonantly by the metal atoms. A small fraction of the scattered light returns to the ground, where it is collected by a telescope and measured by photon-counting. The return signal is electronically binned to give the time delay and hence the height resolution of the scattering layer, typically to within 200 m (Beatty *et al.* 1989). Figure 3 shows an example of a Na lidar return signal. Note how prominent the scattering from the Na layer is compared with the Rayleigh scattering around 30 km, even though the observed Na signal is reduced by about a factor of nine because the scattering layer is three times further from the telescope. The atomic-metal density in the mesosphere is in fact calibrated from the Rayleigh-scattered cross-section at a lower altitude of known atmospheric temperature and density, using the calculated Rayleigh-scattering cross-section (Tilgner and von Zahn 1988). As in the case of the photometric method, the lidar technique relies on the fact that the scattering cross-sections of the metal atoms being studied are much greater than the Rayleigh scattering of the air at the low pressures in the mesosphere.

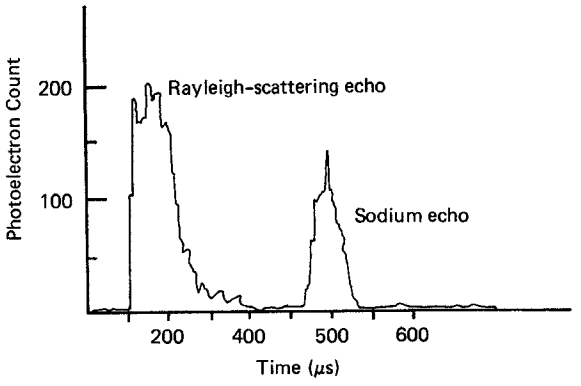

Figure 3. The return signal of a sodium lidar tuned to the D_2 resonance line of atomic Na($3^2P_{3/2}$–$3^2S_{1/2}$) at 589·0 nm. This signal was obtained from 32 laser shots; laser energy about 1 J, repetition rate 0·5 Hz. Note that the photomultiplier receiver is gated for about the first 100 μs. (Re-drawn from Megie and Blamont (1977).)

Lidar has so far been used to observe Na, K, Li, Ca, Ca^+ and Fe (section 2.2). In addition, the spatial variation of the Na layer has been studied both by steerable ground-based lidars (Thomas *et al.* 1976, Clemesha *et al.* 1980), simultaneous measurements by a number of lidars at different sites (Gardner *et al.* 1986a) and a lidar flown in an aircraft (C. S. Gardner, University of Illinois at Urbana–Champaign 1989, personal communitation).

The lidar technique possesses a number of important advantages over the photometric method. The first is that observations can be made continuously over a complete diurnal cycle, provided that a receiving telescope of astronomical quality is employed in order to limit scattered sunlight during the daytime. By contrast, the photometer is limited to daytime or twilight measurements only. The second advantage is that observations can be made relatively rapidly. Clearly, the time taken to build up an acceptable signal-to-noise ratio depends on the power of the dye laser, the scattering cross-section of the metal of interest and its atmospheric concentration, and the receiving power of the telescope in the receiver. For a metal like Ca with extremely low atmospheric densities, signal-averaging times of perhaps 100 min are required (Granier *et al.* 1985). On the other hand, in the case of Na, which is the most easily detected metal, a profile can be obtained with a typical modern lidar every 60 s (Beatty *et al.* 1989). This high time resolution has permitted measurements of short-term perturbations to the metal layers caused by tidal forces (Batista *et al.* 1985, Kwon *et al.* 1987) and gravity waves (Megie and Blamont 1977, Gardner and Voelz 1987), observations of localized enhancements by meteor showers (Hake *et al.* 1972, Megie and Blamont 1977, Clemesha *et al.* 1980) and sightings of the sporadic Na layers that are described in section 2.2 (Clemesha *et al.* 1980, von Zahn *et al.* 1987, Senft *et al.* 1989, Batista *et al.* 1989).

A third advantage of the lidar technique is that, at least in the case of a Na lidar, the temperature in the upper atmosphere can be determined simultaneously. This arises because the degree of blending of the hyperfine structure in the two D lines is very temperature-sensitive, and the mesospheric temperature can be measured to an accuracy of about 5 K by employing a narrow line-width laser as the lidar transmitter to scan across the D lines (Gibson *et al.* 1979, Neuber *et al.* 1988).

The major advantage of the photometric technique has been that it relies on less-temperamental hardware than the high-energy lasers employed in lidar instruments. It is thus more suitable for studies of long-term trends, although, as lasers become more reliable, this advantage is falling away. Both techniques have to employ spectroscopic transitions at wavelengths longer than about 320 nm, because absorption in the Hartley band of ozone prevents optical transmission at shorter wavelengths through the atmosphere (Wayne 1985). This restriction means that some of the most abundant meteoric metals such as Mg cannot be observed from ground-based instruments.

2.1.3. *Mass spectrometry*

There have been several measurements of the concentrations of the positive ions of metals in the upper atmosphere by rocket-borne mass spectrometers (Aiken and Goldberg 1973, Narcisi 1973, Zbinden *et al.* 1975, Hermann *et al.* 1978, Kopp and Hermann 1984). The influence of meteoric activity on the abundance of metallic ions in the mesosphere has been demonstrated by Goldberg and Aiken (1973) and Zbinden *et al.* (1975).

2.2. *Observations of neutral metals in the upper atmosphere*

2.2.1. *Sodium*

The radiation from Na in the upper atmosphere is by far the strongest of any from the metals, so that the vast majority of measurements using both the photometric and lidar techniques have been made for Na. There is general agreement that the column density of Na is about 5×10^9 neutral atoms cm^{-2}, varying up and down by a factor of ten with time and location. A seasonal variation is evident in the observations from both hemispheres, with a maximum about one month before the winter solstice and the minimum near to the summer solstice (Hunten 1967, Megie *et al.* 1978). The variation in mean abundance at low latitudes is only about 25% (Donahue and Blamont 1961, Simonich *et al.* 1979). However, at mid-latitudes, the variation increases to approximately 3 : 1, ranging from about 3×10^9 cm^{-2} in summer to about 10^{10} cm^{-2} in winter (Gardner *et al.* 1986b). This variation is somewhat larger at high latitudes (Hunten 1967). For instance, Gardner *et al.* (1988) recently observed a substantial depletion of Na in the summertime Arctic mesosphere over Svalbard (78°N), obtaining an average abundance during July of about 6×10^8 cm^{-2}. Meanwhile, Henriksen *et al.* (1980) observed a wintertime abundance of $1{\cdot}1 \times 10^{10}$ cm^{-2} using photometric measurements of the twilight emission at the same site. By contrast, the Na nightglow emission exhibits maxima at the equinoxes and therefore appears to be decoupled from the Na layer density (Smith and Steiger 1968, Kirchhoff *et al.* 1979).

There has been some uncertainty over the question of a diurnal variation in the Na column density. The early photometric measurements of dayglow emission generally yielded significantly higher abundances than twilight measurements, and a marked diurnal variation in metal abundance was assumed of about 3 : 1 (Hunten 1967, Gadsden and Purdy 1970). However, more recent work by Burnett *et al.* (1972) and the extension of lidar measurements to the daytime (Clemesha *et al.* 1982, Granier and Megie 1982) have demonstrated the absence of a marked diurnal variation and suggest a systematic error in the dayglow measurements. Granier and Megie (1982) have pointed out that photometric measurements, unlike lidar measurements, are dependent on various atmospheric parameters such as atmospheric and aerosol extinction, total ozone content over large horizontal distances, and the altitude and shape of the stratospheric O_3 and mesospheric Na layers.

The altitude of the peak Na concentration varies between 88 and 91 km, the highest values usually occurring during the local summer (Megie *et al.* 1978). The full width at half-maximum (f.w.h.m.) of the layer averages about 10 km. A striking feature is the very steep top-side gradient with a scale-height of 2–3 km (Sandford and Gibson 1970, Tilgner and von Zahn 1988). Even more surprising, in view of the observed turbulent mixing in the mesosphere, is that the scale-height of the underside of the layer can be extremely small. For example, Tilgner and von Zahn (1988) have measured an average scale-height of $-0{\cdot}4$ km during the winter in the Arctic mesosphere. Figure 4 is a representative winter mean Na profile illustrating these characteristics. This density profile, which contains data averaged over a long duration, does not exhibit marked discontinuities. On the other hand, figure 5 shows a sequence of profiles taken over the course of one night. Although the shape of the profile at any moment in time generally corresponds to the mean profile, there is clearly a rapid variation in the altitude of the layer bottom and evidence of wave-like structures propagating through the layer. Such lidar data can be analysed to obtain information on the dynamical processes in the mesosphere, such as gravity waves and tidal forces (section 2.1.2).

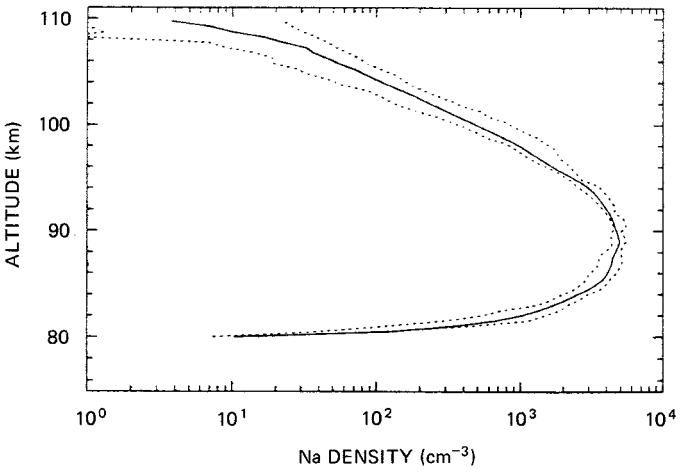

Figure 4. Winter mean Na density profile (solid line) for period December 1985 to February 1986, at 69°N, measured by lidar. Calculated as the median of individual nightly medians, subsequently smoothed with a running mean over 1·5 km altitude. Dashed curves give quartile ranges of the nightly averages. (Reproduced from Tilgner and von Zahn (1988).)

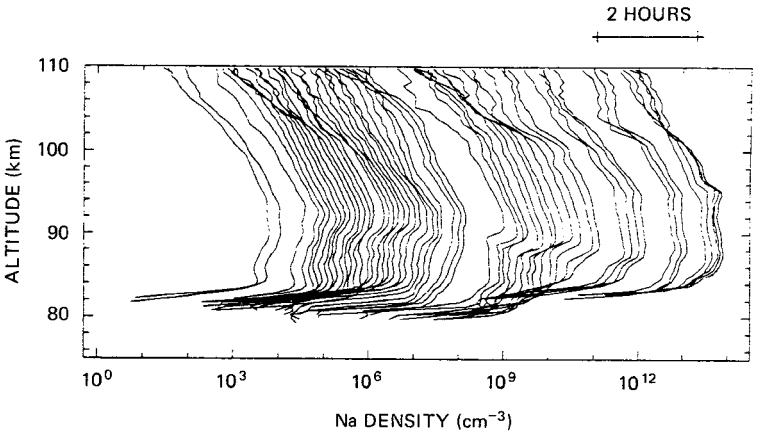

Figure 5. A set of time-resolved Na density profiles measured by lidar over the night 18/19 Janurary 1986, plotted on a logarithmic density scale. Profiles are plotted with a constant offset of 21·12 decades per hour. (Reproduced from Tilgner and von Zahn (1988).)

Lidar measurements of mesospheric Na have recently revealed the dramatic phenomenon of sporadic Na layers (SSLs). These are very thin dense layers of Na, which often form explosively in a matter of minutes, may persist for as long as a few hours, and then disappear rapidly. Figure 6 illustrates the appearance of a typical SSL at 98 km with a f.w.h.m. thickness of about 1 km and a much greater peak density than the normal Na layer at 90 km.

Batista *et al.* (1989) have recently reviewed ten years of Na lidar measurements made at Sao Jose dos Campos (23°S). SSLs were observed about 6% of the time, with an average height of 95 km and an average f.w.h.m. of 2 km. Durations of 1–2 h were typical. The ratio of the maximum SSL peak density to the average Na layer peak density is normally 2·5–3·0, but ratios as high as 7 were occasionally observed. Other

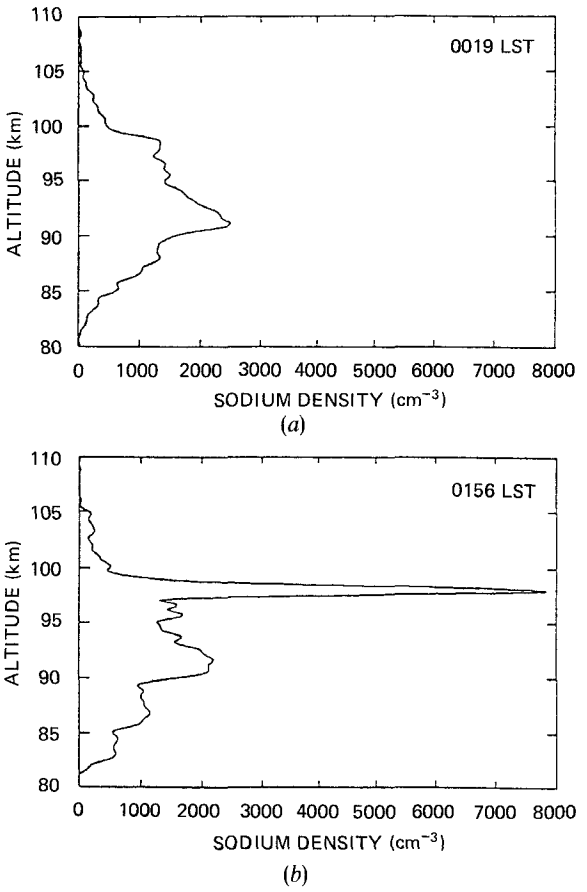

Figure 6. Sodium-density profiles measured by lidar at Urbana on 31 October 1988: (*a*) at 00:19 LST, before the sporadic Na layer appeared, and (*b*) at 01:56 LT, the time at which the sporadic layer reached maximum density. (Reproduced from Senft *et al.* (1989).)

low-latitude observations of SSLs have been made by Kwon *et al.* (1988) at Mauna Kea (20°N) and by Beatty *et al.* (1989) at Arecibo (18°N). At both sites, frequent observations of SSLs were made. This has also been the case at sites of very high latitude such as Andoya (69°N) (von Zahn *et al.* 1987) and Svalbard (78°N) (Gardner *et al.* 1988). However, at the mid-latitude sites at Winkfield (51°N), Observatoire d'Haute Provence (44°N) and Urbana (40°N), not a single SSL event had been reported over two decades of consistent measurements (von Zahn and Hansen 1989) until a very recent observation of a SSL at Urbana (Senft *et al.* 1989). Another puzzling observation is that SSLs mostly occur between 15:00 and 00:00 local time (von Zahn and Hansen 1989, Batista *et al.* 1989).

In a recent experiment at Arecibo, an incoherent scatter radar was deployed simultaneously with a lidar and showed that the presence of a sporadic E layer was closely coupled to the appearance of a SSL (Beatty *et al.* 1989). Strong statistical correlations between sporadic E and SSL formation have also been established in other studies (von Zahn and Hansen 1988, Kwon *et al.* 1988, Batista *et al.* 1989). This evidence has led Beatty *et al.* (1989) to suggest that the sporadic Na layer may be formed through

Na cluster ions being rapidly reduced to Na by the enhanced electron densities characteristic of sporadic E, although the mechanism remains a matter of conjecture.

von Zahn *et al.* (1987) have suggested that the Na in SSLs is liberated from thin dust layers by the action of auroral particle precipitation, but the recent observations of SSLs at low lattitudes precludes this theory as an explanation of SSLs in general. Clemesha *et al.* (1980) have postulated that an SSL could result from the direct deposition of Na from a large meteor. The horizontal transport of the meteor trail across the field of view of the lidar could then account for the rapid growth and decay that is typical of SSLs. This theory was later refined (Clemesha and Simonich 1989) to include the effect of wind shear acting on the trail, as an explanation for the small f.w.h.m. typical of SSLs. However, as von Zahn and Hansen (1988) point out, this theory cannot account for those SSLs that persist for several hours, nor for the greater frequency of SSLs before midnight in contrast with the highest frequency of meteors at 06:00 LT (McSween 1987). In addition, Beatty *et al.* (1988) have actually observed meteor trails with the Urbana lidar. These are unlike SSLs in that they form between 82 and 89 km, last for about 100 s, and are extremely narrow (about 140 m f.w.h.m.). To conclude, the origin of SSLs is one of the most interesting current problems in the aeronomy of the mesosphere.

2.2.2. *Potassium*

The presence of K in the Earth's upper atmosphere was first established by Sullivan and Hunten (1964) from photometric observation of the twilight emission at 766·5 and 769·9 nm. This work was continued by Gault and Rundle (1969). The first lidar measurements of the K layer were made by Felix *et al.* (1973). Megie *et al.* (1978) performed a year-long study where K and Na were measured simultaneously by lidar. The K column density at Observatoire d'Haute Provence (44°N) was about 3×10^8 cm^{-2}, and it remained constant to within a factor of two throughout the year. The absence of a significant winter enhancement in the K column density, in agreement with the photometric study of Gault and Rundle (1969), is particularly striking by contrast with Na (see above). The abundance ratio of these elements (Na/K) thus increases from a low summer value (about 10) to a high winter value (about 50). The altitude of the K peak concentration shows a small seasonal variation similar to that observed for Na, and is on average 1·2 km below the Na peak (Megie *et al.* 1978).

2.2.3. *Lithium*

Lithium was reported to be observed in the twilight emission at 670·8 nm almost simultaneously by Delannoy and Weill (1958) and Gadsden and Salmon (1958). Sullivan and Hunten (1964) showed that during these early measurements the atmosphere had been contaminated by the artificial injection of Li by atomic bomb tests, rendering it difficult to determine with certainty the natural column density of this metal. Jegou *et al.* (1980) carried out a more recent lidar study of Li. The wintertime Li column density at Observatoire d'Haute Provence (44°N) varied within the range $(1{\cdot}5\text{–}3) \times 10^6$ cm^{-2}. This decreased during summer by a factor of about 5, indicating that Li has a slightly larger seasonal variation than Na. As in the case of Na, the wintertime enhancement seems to be greatest in the polar mesosphere, where a column density of $1{\cdot}9 \times 10^8$ cm^{-2} has been observed at Svalbard (78°N) (Henricksen *et al.* 1980). The winter profiles of atomic Li are located around 92 km, roughly 4 km higher

than the wintertime Na peak (Jegou *et al.* 1980). Observers agree that the Li layer exhibits extreme variability: fluctuations in column density exceeding a factor of four have been measured over a single day (Henricksen *et al.* 1986).

2.2.4. *Calcium*

Atomic Ca was first observed in 1985 by lidar (Granier *et al.* 1985). The column density at Observatoire d'Haute Provence (44°N) is $2{\cdot}7 \times 10^7\,\mathrm{cm}^{-2}$ (Granier *et al.* 1989a). This low abundance of Ca accounts for the failure of previous attempts using photometry to measure this metal (Gadsden 1969). The Ca layer is centred at 89 km, and there does not appear to be a systematic seasonal variation of Ca abundance. Granier *et al.* (1985, 1989a) also reported simultaneous measurements of Ca^+ by lidar. On average, the abundance of Ca^+ is lower than that of Ca by a factor of 2·1, and the peak of the Ca^+ layer is at 95 km.

2.2.5. *Iron*

Atomic Fe was first measured by photometric observation of the twilight emission at 386·0 nm by Broadfoot and Johanson (1976). Later photometric measurements by Tepley *et al.* (1981) and Mathews (1981) at Arecibo (18°N) were in agreement that the maximum Fe concentration was $10^9\,\mathrm{cm}^{-2}$. A recent lidar study by Granier *et al.* (1989b) at Observatoire d'Haute Provence (44°N) found somewhat higher abundances. These ranged from $2{\cdot}6 \times 10^9\,\mathrm{cm}^{-2}$ in April to $3{\cdot}6 \times 10^9\,\mathrm{cm}^{-2}$ in November, indicating a modest seasonal variation at mid-latitudes.

2.3. *Summary*

Observations of metals in the upper atmosphere have revealed many intriguing phenomena. These include the appearance of the metal atoms in layers at about 90 km with extremely small scale-heights, the different seasonal behaviours of metals that would be expected to have similar chemistries, such as Na and K, the substantial depletion of Ca relative to Na, and the appearance of SSLs. There is also the fundamental question of whether the source of the metals is both meteoric and terrestrial. Attempts to address these problems have historically been hindered by the fact that observations can only be made of the metal atoms and their ions: no direct information has been available regarding the compounds such as the oxides and hydroxides that these metals are expected to form below 90 km. In the absence of such information from observations, progress can only be made through laboratory studies.

3. Laboratory investigations

Laboratory studies of the atmospheric chemistry of neutral metallic species are relatively recent: the first studies were only published in 1982. This was largely because of the technical difficulties of studying reactions of metallic species in the gas phase at temperatures approaching those found in the mesosphere. Nevertheless, as this section will demonstrate, a number of specialized experimental techniques have now been developed, and a great deal has been accomplished in the last seven years. Section 3.1 contains descriptions of these techniques and lists the atmospherically important metal reactions that have been studied using them. Section 3.2 then provides tables of the temperature-dependent rate coefficients that are recommended for use in atmospheric models. Note that this review does not cover laboratory studies of metal-ion–molecule reactions, which of course date back several decades. The interested reader is directed

to the review by Ferguson and Fehsenfeld (1968) or to general texts on atmospheric chemistry (McEwan and Phillips 1975, Wayne 1985, Brasseur and Solomon 1986).

3.1. *Experimental techniques*

3.1.1. *The flash-photolysis technique*

This technique has been employed in a number of configurations to study metal reactions of atmospheric interest (Husain and Plane 1982a, Plane and Husain 1986, Plane 1987, Husain 1989). A short pulse of ultraviolet light, from a flash lamp or an excimer laser, is used to photolyse a metal-containing precursor in the gas phase. This produces the corresponding metal atoms in an excess of a molecular reactant diluted in a bath gas. The subsequent reaction of the metal atoms is then followed using one of several time-resolved monitoring procedures, which have included laser-induced fluorescence, resonance absorption, and chemiluminescence. These three methods are discussed below.

3.1.1.1. *The two-laser pulse/probe technique*

This is the most recent of the flash photolysis systems to be developed. Figure 7 is a block diagram of the experimental system, which has been described in detail by Plane (1987). Briefly, reactions are studied in a stainless-steel reactor consisting of a central cylindrical reaction chamber at the intersection of two sets of horizontal arms that cross orthogonally. The reactor is shown in figure 8. The arms provide the optical coupling of the lasers to the central chamber where the reactions are initiated, as well as the means by which the flows of the reactants and the bath gas enter the chamber. One of these arms is independently heated to act as a heat-pipe source of the metal precursor vapour. A fifth vertical side-arm provides the coupling for the photomultiplier tube that monitors the LIF signal. The temperature of the central chamber can be varied from 215 to 1100 K. The gas flows enter the side-arms of the reactor close to the optical windows in order to sweep these clear of any metallic species that would otherwise diffuse out of the central chamber.

This system has been used to study reactions of the metals Li, Na, K and Ca. The metal precursors most often used have been the metal iodides, although recently potassium acetate was used in a study of the reaction $K + O_2 + N_2$ (Plane *et al.* 1990). The major advantage of organometallic salts over the metal halides becomes apparent when studying a reaction involving a strong oxidant, such as the recombination reaction between a metal atom and O_2. Plane and Rajasekhar (1988a, b, 1989) have shown that, at temperatures above 400 K, O_2 liberates the molecular halogen (e.g. I_2) from the metal halide on the hot walls of the vessel, which results in a serious kinetic interference. The powdered precursor salt is placed in a tantalum boat in the heat pipe (figure 8), and then carefully heated to a temperature where the equilibrium vapour pressure of the precursor above the salt in the boat is about 10^{13} cm^{-3}. This vapour is then entrained in a flow of the bath gas and carried into the central chamber, where it can be photolysed using either an excimer laser at 193 nm (Plane *et al.* 1990) or a small flash lamp (Plane and Rajasekhar 1988b).

The resulting metal atoms are probed by exciting fluorescence from a strongly allowed transition using a nitrogen-pumped dye laser of narrow bandwidth (approximately 0·01 nm). The detection limit of a metal atom such as Li is estimated to be about 10^7 cm^{-3} in this system.

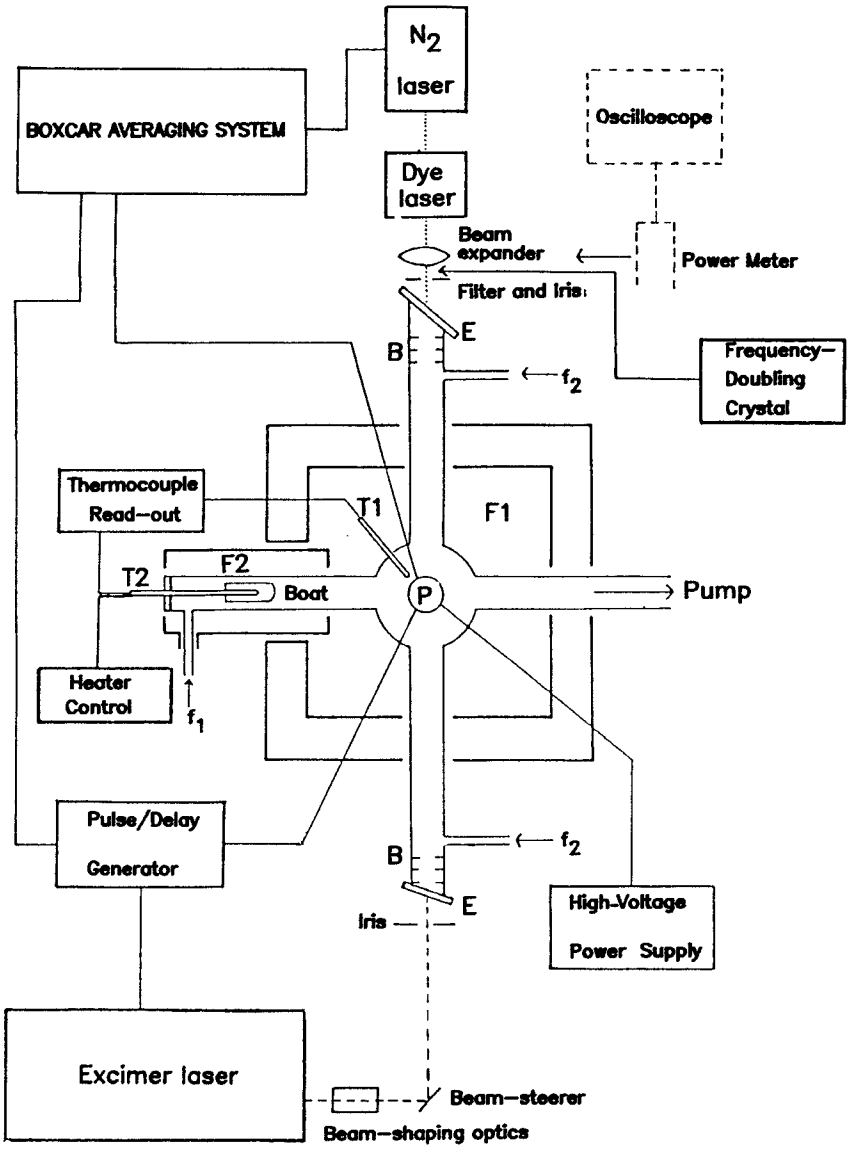

Figure 7. Block diagram of the two-laser pulse/probe system. Components are identified as follows: B, baffle to reduce scattered light; E, suprasil end window set at the Brewster angle; F1, furnace around the central chamber of the reactor; F2, furnace around the heat pipe; f_1, flow of bath gas; f_2, flow of reactant diluted in bath gas; P, photomultiplier tube; T1, thermocouple in the central chamber; T2, thermocouple in the heat pipe.

The laser-induced fluorescence signal passes through an appropriate interference filter before being recorded by the photomultiplier, whose output is then captured by the gated integrator of a boxcar averager. The probe laser is triggered by the boxcar to coincide with the opening of the integrator gate as it is scanned to monitor the LIF signal at increasing time intervals after the excimer laser fires.

Experiments are conducted so that the metal atoms are always in a large excess of the molecular reactant, and hence the kinetic disappearance of the metal atoms is

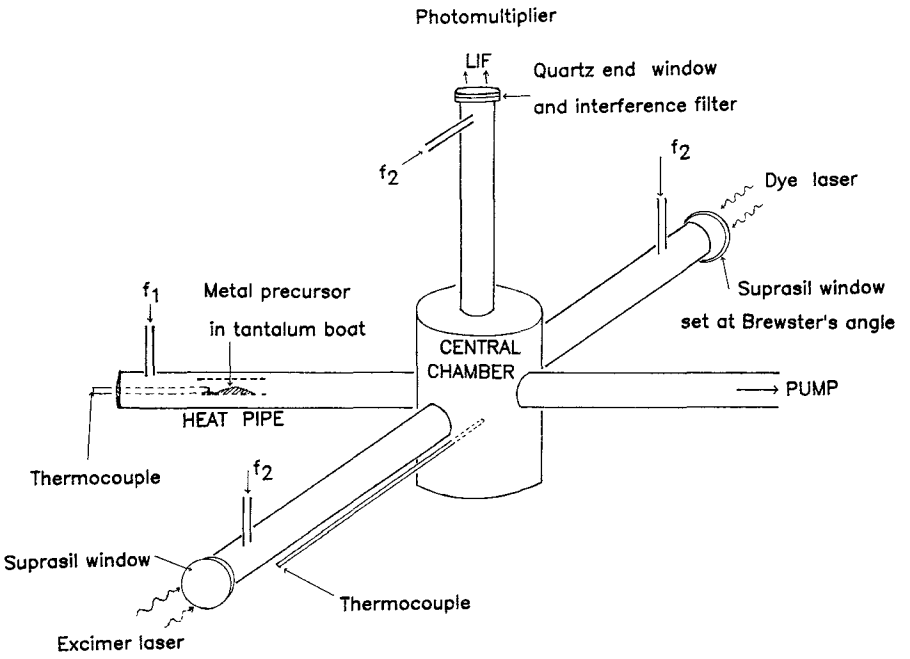

Figure 8. Diagram of the reactor in the two-laser pulse/probe system. Components are identified as follows: f_1, flow of bath gas; f_2, flow of reactant diluted in bath gas; LIF, laser-induced fluorescence signal.

pseudo-first-order. The decay of the LIF signal, which is proportional to the metal-atom concentration, should then be a simple exponential. Figure 9 shows examples of the decays of Li atoms in an excess of O_2 and a third body (N_2 or He) at 267 K. The parts of this figure show how the loss of Li depends on both $[O_2]$ and the third-body concentration, as expected for a termolecular reaction. Notice that N_2 is roughly twice as efficient as He as a third body. Details of the extraction of rate coefficients from such kinetic decays are given in Plane and Rajasekhar (1988b). Diffusive loss, out of the volume in the centre of the chamber produced by the intersection of the photolysis and probe beams, limits the slowest pseudo-first-order chemical processes that may be observed with this system to about $100\,s^{-1}$. Because of a 1·2 μs firing delay of the dye laser, the fastest decays that can be recorded are about $10^5\,s^{-1}$.

Sometimes the kinetic decays at high temperatures exhibit an approach to equilibrium of the reaction. Under appropriate circumstances, the calculated equilibrium constants can then be used, together with statistical mechanics, to derive bond energies of metallic species that are otherwise only poorly known (Plane and Rajasekhar 1988a). In the case of the recombination reactions between the alkali atoms and O_2, which do not significantly approach equilibrium even at 1100 K, lower limits to their bond energies were obtained in this way. These lower limits were then combined with *ab initio* calculations to yield recommended bond energies (Plane *et al.* 1989a, 1990).

An important application of the two-laser pulse/probe system to mesospheric metal chemistry has been to study the recombination reactions of Li, Na and K with O_2 over the temperature range 230–1120 K (Plane and Rajasekhar 1989b, 1989, Plane *et al.* 1990). Figure 10 illustrates the results of these three studies. The tremendous advantage of being able to study reactions over such a broad range of temperature is that rate

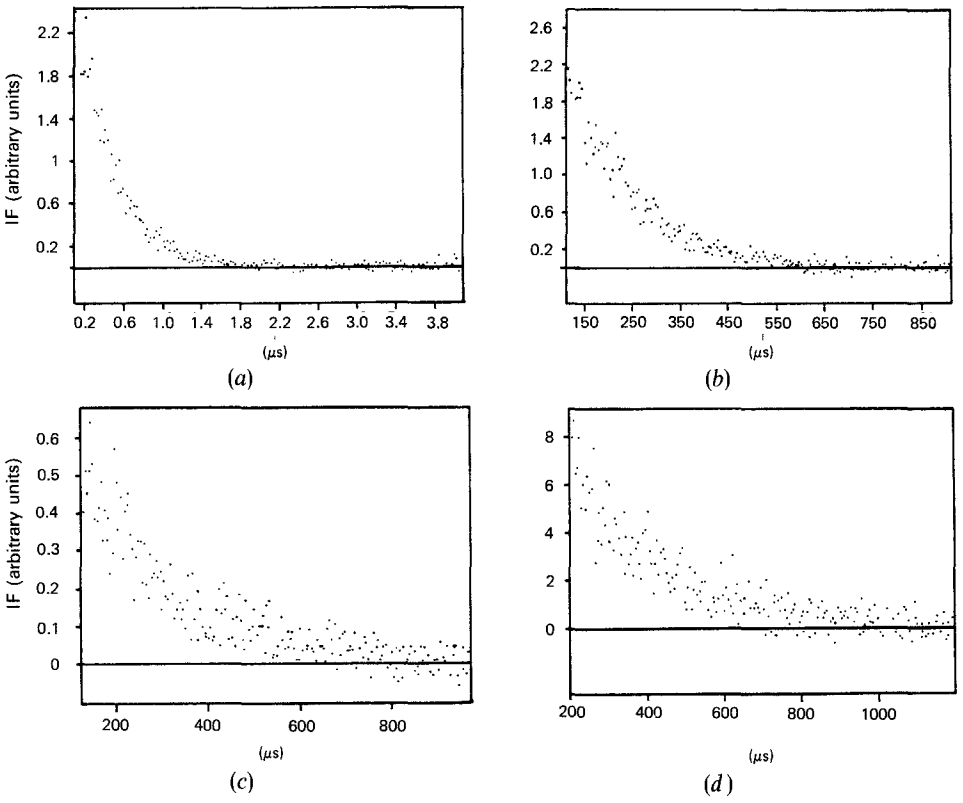

Figure 9. Time-resolved decay of the LIF signal from Li atoms at 670·7 nm ($Li(2^2P_J)$–$Li(2^2S_{1/2})$) following the pulsed photolysis of LiI vapour at $T=267$ K: (*a*) $[O_2]=1{\cdot}5\times10^{15}$ cm^{-3}, $[N_2]=3{\cdot}6\times10^{17}$ cm^{-3}; (*b*) $[O_2]=4{\cdot}5\times10^{15}$ cm^{-3}, $[N_2]=3{\cdot}6\times10^{17}$ cm^{-3}; (*c*) $[O_2]=1{\cdot}1\times10^{15}$ cm^{-3}, $[N_2]=5{\cdot}4\times10^{17}$ cm^{-3}; (*d*) $[O_2]=4{\cdot}3\times10^{15}$ cm^{-3}, $[He]=5{\cdot}4\times10^{17}$ cm^{-3}. (Reproduced from Plane and Rajasekhar (1988).)

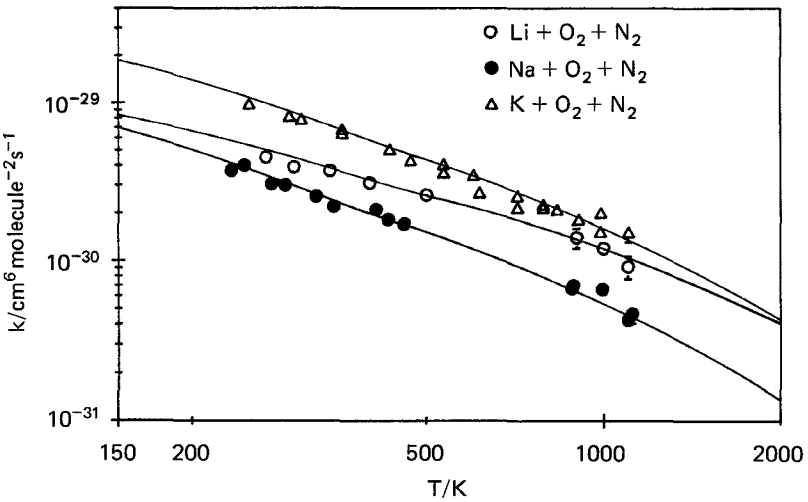

Figure 10. Logarithmic plots of the termolecular rate coefficient k against T for the reactions Li, Na and $K + O_2 + N_2$ (data taken from Plane and Rajasekhar (1988b, 1989) and Plane *et al.* (1990)). The solid lines are extrapolations of the experimental data for each reaction to the temperature range 150–2000 K, using the Troe (1977) formalism.

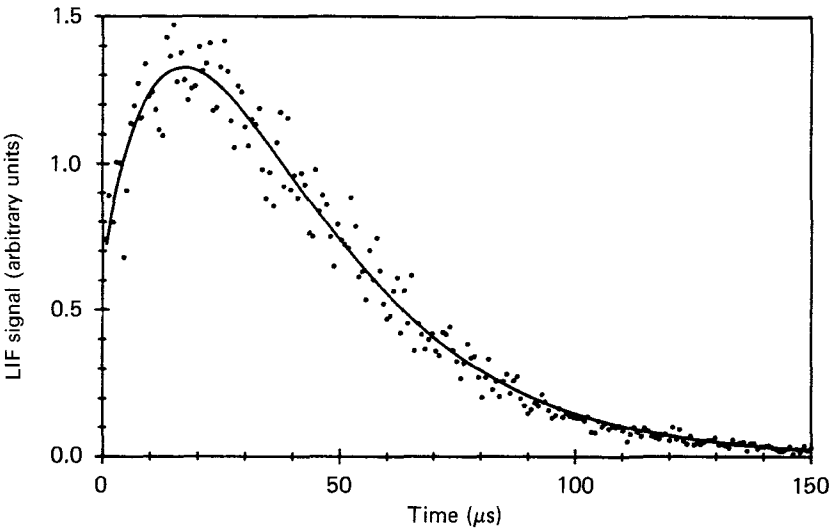

Figure 11. Time-resolved variation of the LiF signal at 422·7 nm [$Ca(^1P_1)$–$Ca(^1S)$], following the pulsed photolysis of CaO/N_2O in He at 193·3 nm; reactor temperature 805 K; $[N_2O] = 1{\cdot}1 \times 10^{15}\,cm^{-3}$; $[CaO] = 1{\cdot}3 \times 10^{14}\,cm^{-3}$; $[He] = 6{\cdot}1 \times 10^{16}\,cm^{-3}$. The solid line through the experimental data is a fitted solution to the differential equation describing the chemistry: $CaO + O \rightarrow Ca + O_2$ and $Ca + N_2O \rightarrow CaO + N_2$.

coefficients can then be extrapolated with greater confidence to extremely low temperatures that are not amenable to experimental study. In the case of termolecular reactions, the Troe formalism (Troe 1977) is now an established way for doing this (DeMore *et al.* 1985). The formalism is based on a simplified form of RRKM theory (Smith 1980), only requiring for input the molecular parameters of the molecule formed in the recombination process and a measured value of the recombination rate coefficient at some temperature. The solid lines in figure 10 show a very satisfactory fit of the Troe formalism through the experimental points for each reaction, enabling the rate coefficients to be calculated over the mesospheric temperature range (Plane *et al.* 1990).

In a very recent study with this system, the atmospherically important reaction $CaO + O$ was measured (Plane and Nien 1990). Ca vapour was flowed from the heat pipe and mixed with an excess of N_2O in the central reactor to form CaO. Photolysis of the CaO and excess N_2O then produces $O(2^3P_J)$ atoms, which react with the CaO to produce Ca atoms. Thus an initial growth of the Ca concentration is observed, followed by a decay at longer times as the Ca reacts with the excess N_2O. This is shown in figure 11. In this experiment, small residence times in the reactor were employed to avoid condensation of CaO on the walls (contrast section 3.1.1.3). Although elevated reactor temperatures were required, this reaction is extremely rapid and so it can be extrapolated with confidence to mesospheric temperatures.

The two-laser technique has also been used to measure the absolute photolysis cross-section of NaO_2 (Rajasekhar *et al.* 1989). In this experiment, the superoxide is made by titrating Na vapour with O_2. The NaO_2 is then photolysed by an excimer laser beam of known fluence, and the degree of photolysis is calculated by measuring the resulting Na atoms by LIF a few microseconds after the excimer pulse. This procedure for determining the absolute cross-section was originally developed by Silver *et al.*

(1985) and is discussed further below. Rajasekhar *et al.* (1989) also found evidence for the production of sodium tetroxide NaO_4 in the gas-phase at 230 K from the addition of O_2 to NaO_2. The possible importance of the tetroxide is discussed in section 5.

3.1.1.2. *The flash-photolysis/resonance-absorption technique*

This technique was developed by Husain and Plane (1982a) and is illustrated in figure 12. The design of the experiment followed the pioneering work of Davidovits (1979). The reactor is a quartz absorption cell about 2 cm in diameter and 20 cm long, in which an alkali-halide salt is placed. Adjacent and parallel to this cell is a high-energy (250 J) quartz flash lamp. Both the cell and flash lamp are enclosed in a furnace, which can heat them to over 1000 K. Condensation of the salt vapour on the end windows of the cell is avoided by insulating them with evacuated extensions that keep them at the same temperature as the centre of the cell. Gases are admitted to the cell through a magnetically controlled valve, which is normally closed to prevent escape of the halide vapour from the cell. The experiment is initiated by photolysing the alkali-iodide vapour to produce the metal atoms in a pseudo-first-order excess of a molecular reactant. The attenuation of the concentration of the metal atoms due to diffusion to the walls and chemical reaction is monitored by resonance absorption, using a purpose-built high-intensity alkali resonance lamp (Husain and Plane 1982a, b, Husain *et al.* 1985a, b, 1986). The light from the resonance lamp is directed through the cell and focused on to the slits of a monochromator that discriminates the resonance wavelength from the continuum of scattered light from the flash lamp. The time-resolved attenuation of the resonance lamp is then monitored by a photomultiplier attached to the monochromator and the signal is captured by a transient recorder. These experiments were performed in the 'single-shot' mode, so that degrees of absorption in excess of 5% were required for reasonable signal-to-noise levels. Thus the detection limit for Na atoms in this system is about $10^9\,cm^{-3}$. The question of the adherence of the Beer–Lambert law at these relatively high degrees of absorption, and the empirical corrections that may be required to extract kinetic information, are discussed by Husain and Plane (1982a, b).

Rate coefficients are obtained in the same manner as described above (section 3.1.1.1). The most rapid first-order decays that can be measured are about $2500\,s^{-1}$, determined by the recovery of the PMT following the pulse of scattered light from the large flash lamp. This system has been employed to study a number of atmospherically important reactions of Na and K, albeit at temperatures in excess of 400 K where the alkali-iodide vapour pressure in the cell is large enough to obtain measurable absorbances upon photolysis. These reactions have included the recombination of Na and K with O_2 to give the alkali superoxides (Husain and Plane 1982a, b, Husain *et al.* 1985a, 1986, 1987), and the reaction between Na and O_3 (Husain *et al.* 1985b).

3.1.1.3. *The flash-photolysis/chemiluminescence technique*

This technique was employed by Plane and Husain (1986) to study the reaction $NaO + O \rightarrow Na(^2P, ^2S) + O_2$, by using the chemiluminescence from the $Na(3^2P_J)$ product as a spectroscopic marker of the reaction. $O(2^3P_J)$ atoms were produced by the pulsed photolysis of NaO, itself produced *in situ* by adding N_2O to an excess of Na vapour. This reaction was carried out in a stainless-steel reactor, to which was coupled a heat-pipe oven, shown in figure 13. Further details of the reactor can be found in Husain *et al.* (1984). The Na vapour produced in the heat-pipe oven was monitored by steady atomic resonance fluorescence at 589 nm using phase-sensitive detection. The

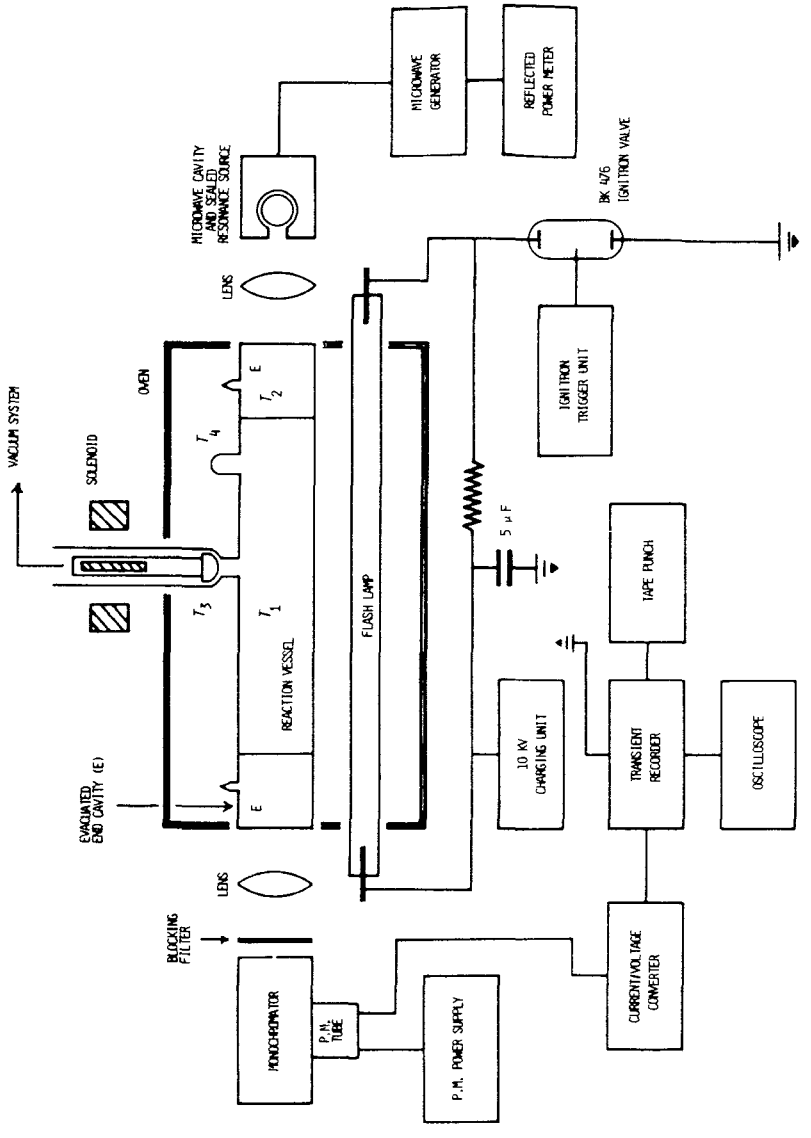

Figure 12. Block diagram of the apparatus for the kinetic study of $Na(3^2S_{1/2})$ by time-resolved atomic resonance absorption spectroscopy in the single-shot mode following pulsed irradiation. (Reproduced from Husain and Plane (1982).)

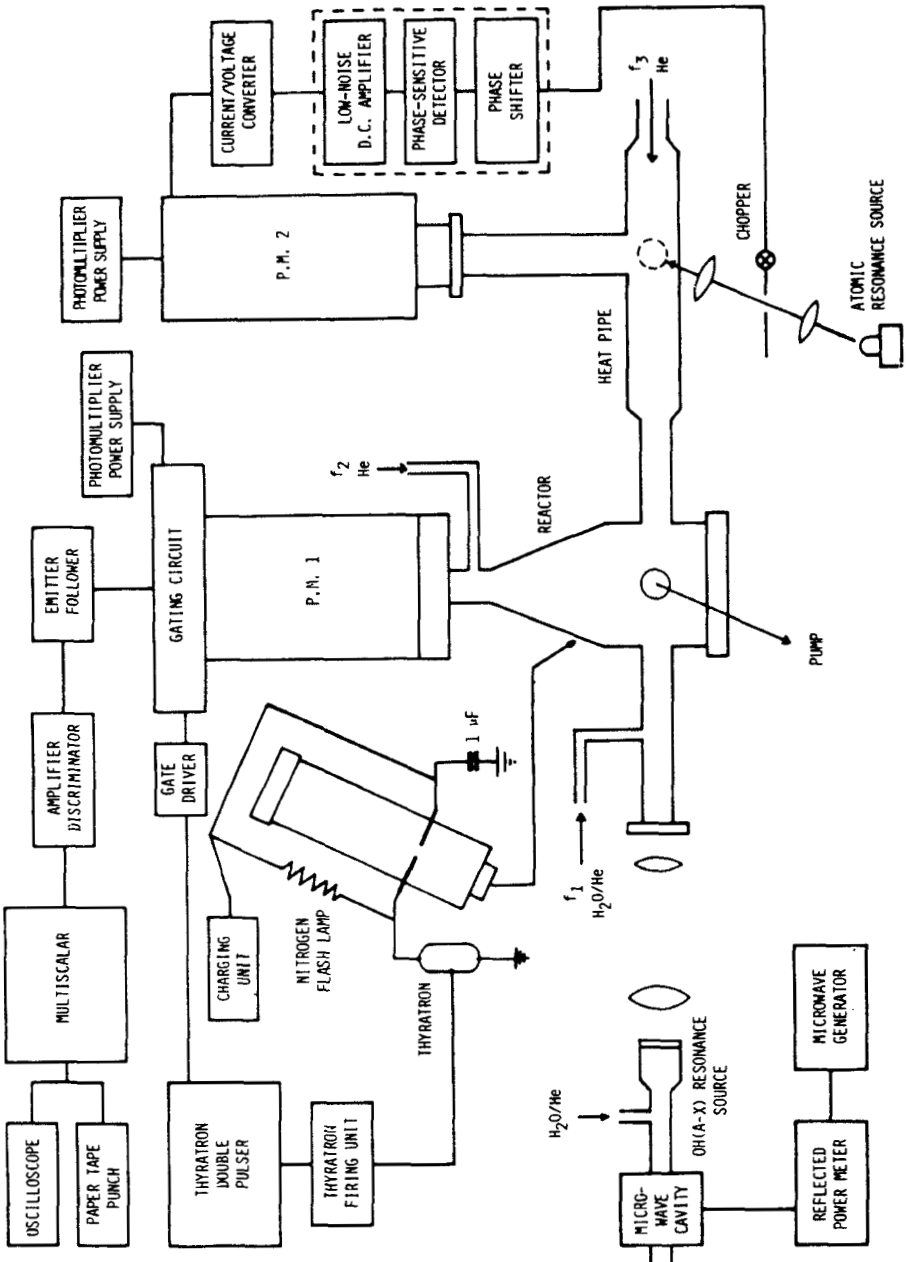

Figure 13. Block diagram of the apparatus for the kinetic study of the reaction $NaO + O \rightarrow Na(^2P, ^2S) + O_2$, employing (*a*) time-resolved chemiluminescence measurements from $Na(^2P)$ at 589 nm following the pulsed photolysis of NaO, and (*b*) steady resonance fluorescence at 589 nm coupled with phase-sensitive detection on atomic Na derived from a heat-pipe oven. (Reproduced from Husain *et al.* (1984).)

Na vapour was then flushed with He bath gas from the oven into the reactor, where it mixed with a flow of N_2O. Na and N_2O react together very rapidly at elevated temperatures to form NaO (Plane and Rajasekhar 1989). The steady-state concentration of NaO in each experiment was subsequently calculated from the measured input of N_2O into the reactor and the diffusion of NaO out of the effectively cylindrical reactor using the 'long-time' solution of the diffusion equation for a cylinder (Mitchell and Zemansky 1961). The NaO concentration could thus be altered by changing the flow of N_2O, and maintaining the Na in excess. To avoid uncertainties caused by the loss of Na on the reactor walls, the reactor was kept at 573 K during these experiments. Even though this temperature is well above ambient mesospheric temperatures, this reaction turned out to be extremely fast and could thus be extrapolated with confidence to lower temperatures.

3.1.2. *The fast-flow-tube technique*

In this technique, the time resolution required to make kinetic measurements is obtained by setting up a rapid flow of reactants along a flow tube from an upstream point of injection to a downstream observation point where one of the reactants is monitored. This reactant is arranged to be in a pseudo-first-order excess of the other reactants, and the rate of reaction is then measured by changing the distance between the injection and observation points, and hence the reaction time. The fast-flow-tube technique has been fruitfully applied to studying metal reactions of atmospheric interest by several groups (Fontijn *et al.* 1977, Sridharan *et al.* 1979, Silver *et al.* 1984b, Talcott *et al.* 1986).

Figure 14 shows the essential features of a flow tube designed for studying reactions of Na species (Talcott *et al.* 1986). For additional designs, the reader is referred to Gersh *et al.* (1981) and Silver *et al.* (1984a, 1985). The tube is about 5 cm in diameter and about 70 cm long. It is pumped by a large displacement booster system (500 litres s^{-1}) in order to produce high flow velocities $\geqslant 7\,m\,s^{-1}$ in the tube. The flange at the upstream end contains two movable inlets. The larger inlet carries a flow of Na vapour from an oven

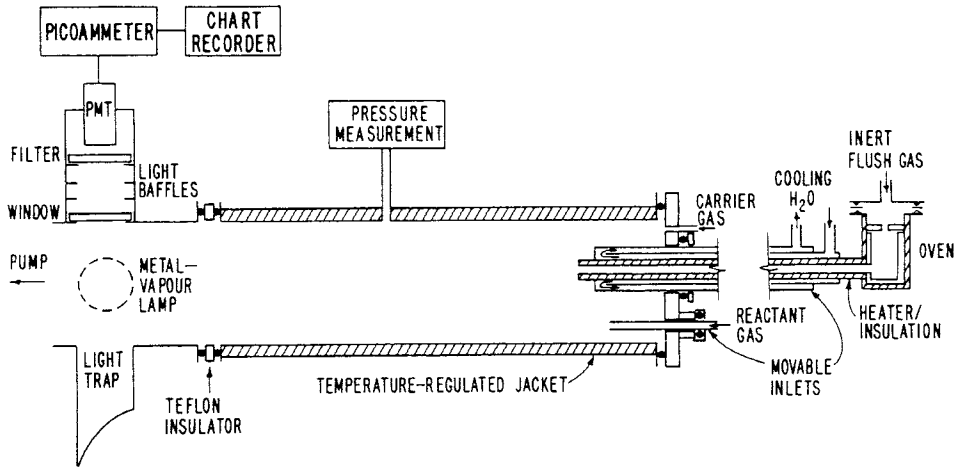

Figure 14. Sodium flow tube with oven source and movable inlets, including detection of atomic Na by steady-resonance fluorescence spectroscopy at 589 nm. (Reproduced from Talcott *et al.* (1986).)

into the flow tube; the smaller inlet is for the injection of other reactants. The carrier gas, which is a large flow of inert gas that is used to establish laminar flow conditions in the tube and decrease the rate of diffusion of reactive species on to the walls of the tube, is also admitted through this flange. The flow tube operates over the temperature range 240–430 K. This is achieved by wrapping copper tubing around the tube, through which a thermostatted liquid is pumped. Na metal is placed in the oven, which is typically heated to 400 K. A small flow of an inert gas then entrains the metal vapour and flushes it down the inlet to the point of injection. This inlet is heated to about 490 K to prevent condensation of the metal, and surrounded by a water-jacket in order to pass through an O-ring seal set into the flange.

Na is detected by resonance fluorescence using a low-pressure Na lamp as the excitation source. The fluorescence signal is measured with a cooled photomultiplier positioned orthogonally to the axis of the lamp. By careful baffling and use of a light trap to reduce scattered light, a detection limit for Na of $10^4\,cm^{-3}$ is estimated.

Talcott *et al.* (1986) have discussed the standard treatment of the continuity equation describing the loss of a reactant, through both chemical reaction in the gas phase and diffusion on to the walls, in a cylindrical tube under laminar flow conditions. Clearly, when studying a metallic species where sticking on the flow tube walls is a major loss component, the correct treatment for wall losses and the resulting radial concentration gradients is crucial.

An important application of the flow-tube technique has been for studying the reactions of Na compounds such as NaO, NaO_2, NaOH and NaCl. These have been made at the upstream end of the flow tube by titrating the Na flow with N_2O (Silver *et al.* 1984a, Ager and Howard 1986, 1987, Ager *et al.* 1986), O_2 (Silver *et al.* 1984b), H_2O_2 (Silver *et al.* 1984a), or Cl_2 (Silver *et al.* 1985). The other reactant is then added further downstream. Na compounds are detected by titration back to Na just upstream of the observation point, by adding a large concentration of a suitable species. For example, NO or CO is used for detecting NaO (Silver *et al.* 1984a, Ager *et al.* 1986, Ager and Howard 1986, 1987), and atomic H has been used for measuring NaOH and NaO_2 (Silver *et al.* 1984a, Silver and Kolb 1986).

The flow-tube technique has been used to study a wide variety of metal reactions of mesospheric and stratospheric interest. Reactions of metal atoms include the recombination of Na and K with O_2 to form their superoxides (Silver *et al.* 1984b), the reaction between Al and O_2 (Fontijn *et al.* 1977, Sridharan *et al.* 1979), and the reaction between Na and O_3 (Ager *et al.* 1986, Silver and Kolb 1986). The reactions of NaO have been studied with O_3 (Ager *et al.* 1986), with H_2 and H_2O (Ager and Howard 1987), with O_2 and CO_2 (Ager and Howard 1986) and with HCl (Silver *et al.* 1984a). The reaction of NaO_2 has been studied with HCl (Silver and Kolb 1986). Lastly, the reactions of NaOH have been studied with H and HCl (Silver *et al.* 1984a) and with CO_2 (Ager 1986).

Silver *et al.* (1985) have used a small flow tube to measure the absolute photolysis cross-section of NaCl, which was made by the reaction $Na + Cl_2$. Figure 15 is a block diagram of the apparatus. The Na concentration was first measured by LIF before Cl_2 was added. Then, after titrating the Na with Cl_2, the NaCl was photolysed using an excimer laser and the resulting Na atoms detected by LIF immediately following the excimer pulse. The ratio of the two LIF signals, divided by the excimer laser-beam fluence, essentially gives the absolute cross-section at the excimer wavelength. Silver *et al.* (1985) also Raman-shifted their excimer laser in order to measure the photolysis cross-section over many UV wavelengths. The resulting photodissociation spectrum is

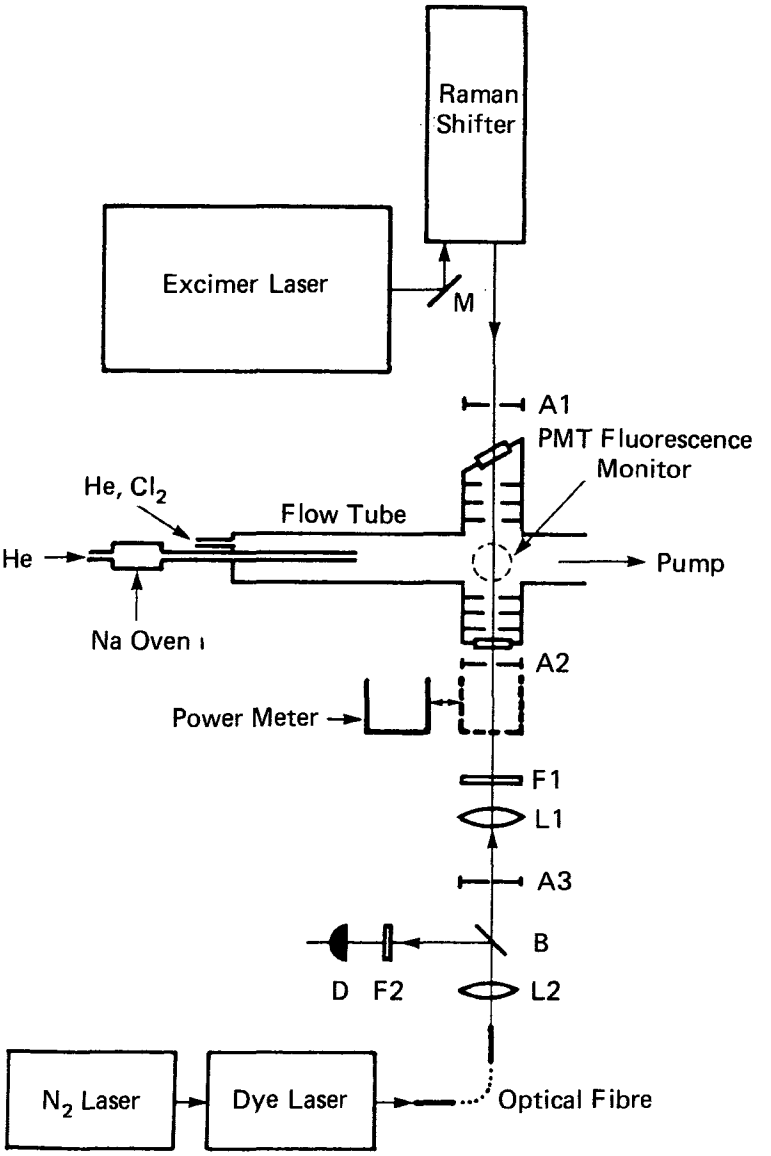

Figure 15. Block diagram of the experimental apparatus for measuring the absolute photodissociation cross-section of NaCl. Components are identified as follows: M, mirror; A1, A2, A3, apertures; F1, BK-7 window acting as a UV absorbing filter; F2, 590 nm interference filter; L1, L2, lenses; B, quartz slide acting as a beamsplitter; D, fast ultraviolet photodiode detector. (Reproduced from Silver *et al.* (1985).)

shown in figure 16. The great advantage of this procedure is that the absolute NaCl concentration is not required to obtain the absolute cross-sections.

Plane (1989) has recently reported a preliminary study of the reaction $NaO_2 + O$, using a new flow-tube reactor similar in design to that of Talcott *et al.* (1986). Although this study is preliminary, the result is included here because of the importance of this reaction to the chemistry of neutral Na below 90 km.

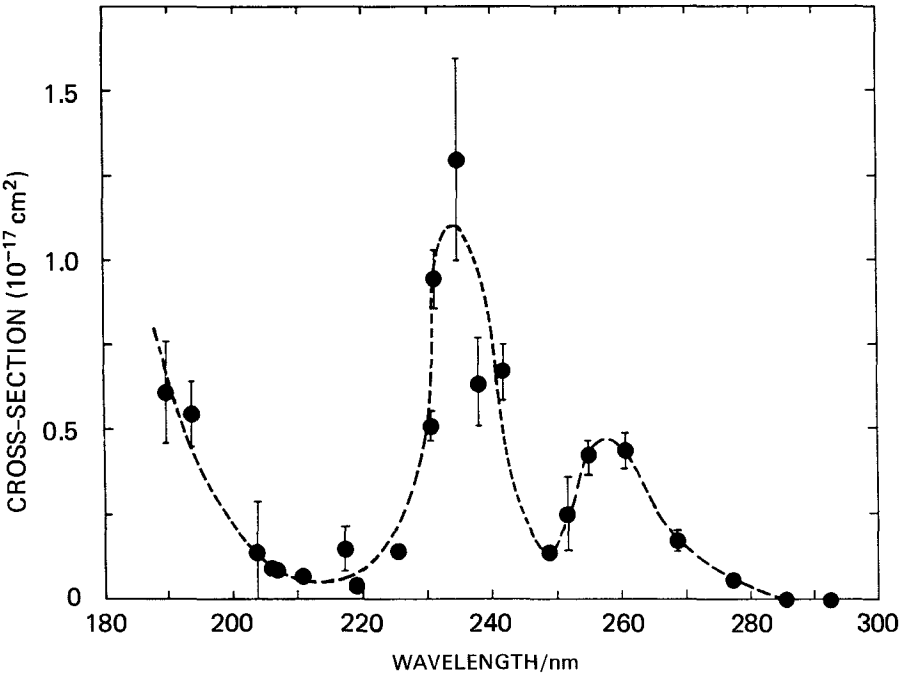

Figure 16. Plot of experimental photodissociation cross-sections against wavelength for NaCl at 300 K. Error bars represent one standard deviation. A dashed curve is drawn through the points to highlight the shape of the data. (Reproduced from Silver *et al.* (1985).)

3.1.3. *Comparison between the experimental techniques*

It should be clear from the above discussion that a significant quantity of kinetic data has been measured with these very different techniques. In general, the flash-photolysis and flow-tube methods each offer exclusive advantages over the other for studying different kinds of reactions (Smith 1980), and the field of low-temperature metal reactions bears these out. The advantages of the flash-photolysis method include the absence of significant wall effects, the ability to study recombination reactions over large ranges of pressure, and the ability to study reactions of refractory metals by photolysing their more volatile organometallic compounds. The major advantage of the fast-flow-tube technique is the ability to study the reactions of metal compounds, which are made in the first section of the tube and then detected at the observation point by reduction back to metal atoms. Such reactions can only be studied under special circumstances in flash-photolysis experiments.

Naturally, however, one would like some intercomparison between these techniques, and this has been provided by the reaction $Na + N_2O$. This reaction exhibits simple Arrhenius behaviour over the temperature range 250–900 K and is not susceptible to systematic errors. It has thus become a 'kinetic standard' for the development of new experimental systems for metal reactions. Figure 17 is an Arrhenius plot for this reaction, indicating the results obtained from the two-laser pulse/probe apparatus (Plane and Rajasekhar 1989), the flash-photolysis/resonance-absorption system (Husain and Marshall 1985) and two flow-tube studies (Silver and Kolb 1986, Ager *et al.* 1986). The agreement between the four studies is extremely good.

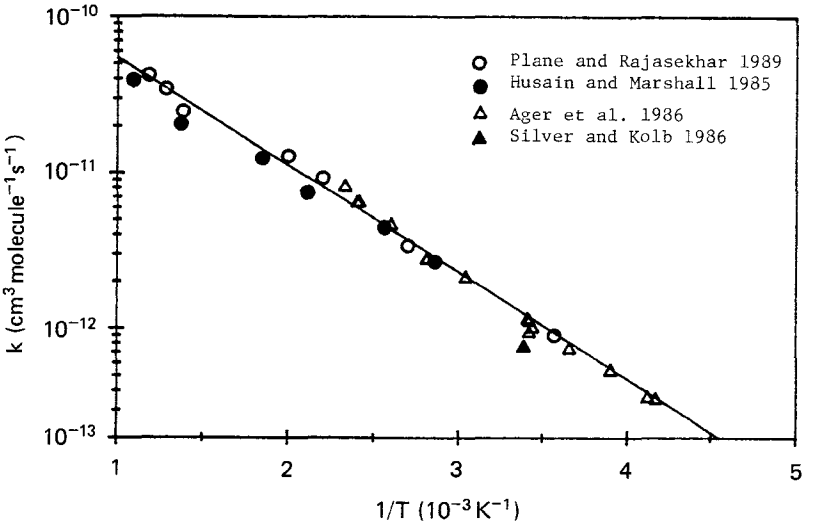

Figure 17. Standard Arrhenius plot over the temperature range 200–1000 K for the reaction $Na + N_2O$. The solid line is a best fit through the data of Plane and Rajasekhar (1989).

3.2. *Recommended rate coefficients*

Table 1 contains a list of the rate coefficients of metal reactions of atmospheric interest that have been measured directly by the techniques described above. The rates of photolysis reactions are also included. The temperature range reported in each study is listed. In the mesosphere, the temperature ranges from 120 to 220 K (CIRA 1972), which is lower than the temperatures actually reached in these experimental studies. However, estimates of the rate coefficients at mesospheric temperatures are required for modelling purposes, and so appropriate expressions are given in table 1. If a temperature-dependent expression for the rate coefficient was reported in the original paper, this is given in the table. Otherwise, bimolecular reactions that proceed at close to the collision number are assigned a $T^{1/2}$ dependence. For slower reactions, the activation energy E_{act} is estimated from the Arrhenius expression $Z\exp(-E_{act}/RT)$. The pre-exponential factor Z is assumed to be equal to the collision number, which is often the case for reactions of atoms and small radicals (Smith 1980). The collision number is calculated from the expression $Z = \sigma(8RT/\pi\mu)^{1/2}$, where σ is the reaction cross-section, R is the gas constant and μ is the reduced mass of the colliding pair. A 'typical' reaction cross-section of 60 Å^2 has been chosen to correspond to the pre-exponential factor for the reaction $Na + N_2O$ (Plane and Rajasekhar 1989). Ter-molecular reactions that were not studied as a function of temperature are assigned a T^{-1} dependence, typical of such processes (Plane *et al.* 1990).

Few of the reactions have been studied by more than one group. In the case of the recombination reactions of Na and K with O_2, Plane and Rajasekhar (1989) and Plane *et al.* (1990) have argued that the inconsistencies between results with different third bodies in some of the flow tube data of Silver *et al.* (1984b) cast doubt on those measurements, and so the more recent flash-photolysis studies are preferred. In the case of the reaction $Na + O_3$, the study by Ager *et al.* (1986) is recommended in preference to both the approximate study of Husain *et al.* (1985b) and the work of Silver and Kolb (1986), which has now been revised to a higher value (Worsnop *et al.* 1989), consistent with that of Ager *et al.* (1986).

Table 1. Rate coefficients for reactions of metal species of atmospheric interest.

Reaction	Temperature range of experiment (K)	$k(T)$ (cm^3 molecule^{-1} s^{-1})	Reference
1. *Bimolecular reactions*			
$Na + O_3 \rightarrow NaO + O_2$	500	$(2{\cdot}5^{+2{\cdot}5}_{-1{\cdot}3}) \times 10^{-10} (T/200\,K)^{1/2}$	Husain *et al.* (1985)
$\rightarrow NaO_2 + O$	300	$(2{\cdot}5 \pm 0{\cdot}3) \times 10^{-10} (T/200\,K)^{1/2}$	Silver and Kolb (1986)
	286	$(6{\cdot}0 \pm 1{\cdot}2) \times 10^{-10} (T/200\,K)^{1/2}$	Ager *et al.* (1986)
Remarks: the major product (>95%) is NaO. The study by Ager *et al.* (1986) is recommended.			
$NaO + O \rightarrow Na(^2P, ^2S) + O_2$	573	$(2{\cdot}2 \pm 0{\cdot}5) \times 10^{-10} (T/200\,K)^{1/2}$	Plane and Husain (1986)
$NaO + O_3 \rightarrow NaO_2 + O_2$	296	$(1{\cdot}5 \pm 0{\cdot}3) \times 10^{-10} (T/200\,K)^{1/2}$	Ager *et al.* (1986)
$\rightarrow Na + 2O_2$	296	$\approx 3{\cdot}2 \times 10^{-10} \exp(-550\,K/T)$	Ager *et al.* (1986)
$NaO + H_2 \rightarrow NaOH + H$	296	$(1{\cdot}1 \pm 0{\cdot}2) \times 10^{-9} \exp(-1100\,K/T)$	Ager and Howard (1987)
$\rightarrow Na + H_2O$	296	$\approx 1{\cdot}1 \times 10^{-9} \exp(-1400\,K/T)$	Ager and Howard (1987)
$NaO + H_2O \rightarrow NaOH + OH$	298	$(1{\cdot}8 \pm 0{\cdot}3) \times 10^{-10} (T/200\,K)^{1/2}$	Ager and Howard (1987)
$NaO + HCl \rightarrow NaCl + OH$	308	$\approx 2{\cdot}3 \times 10^{-10} (T/200\,K)^{1/2}$	Silver *et al.* (1984a)
$NaO_2 + HCl \rightarrow NaCl + HO_2$	295	$(1{\cdot}9 \pm 0{\cdot}3) \times 10^{-10} (T/200\,K)^{1/2}$	Silver and Kolb (1986)
$NaOH + HCl \rightarrow NaCl + H_2O$	308	$(2{\cdot}3 \pm 0{\cdot}7) \times 10^{-10} (T/200\,K)^{1/2}$	Silver *et al.* (1984a)
$CaO + O \rightarrow Ca + O_2$	805	$(3{\cdot}2 \pm 1{\cdot}1) \times 10^{-10} (T/200\,K)^{1/2}$	Plane and Nien (1990)
$Al + O_2 \rightarrow AlO + O$	310	$(3{\cdot}0 \pm 0{\cdot}8) \times 10^{-11} \exp[-(18 \pm 80)\,K/T)]$	Fontijn *et al.* (1977)
	300	$2{\cdot}4 \times 10^{-11}$	Sridharan *et al.* (1979)
2. *Termolecular reactions* (with N_2 as third body)			
$Na + O_2 \rightarrow NaO_2$	233–1118	$(4{\cdot}7 \pm 0{\cdot}5) \times 10^{-30} (T/200\,K)^{-1{\cdot}22}$	Plane and Rajasekhar (1989)
	416–1016	$(8{\cdot}3 \pm 0{\cdot}5) \times 10^{-30} (T/200\,K)^{-1{\cdot}42}$	Husain *et al.* (1986)
	320–700	$(3{\cdot}0 \pm 0{\cdot}6) \times 10^{-30} (T/200\,K)^{-1{\cdot}1}$	Silver *et al.* (1984b)
Remarks: the result of Plane and Rajasekhar (1989) is recommended (see text)			
$NaO + O_2 \rightarrow NaO_3$	297	$(5{\cdot}3 \pm 1{\cdot}2) \times 10^{-30} (T/200\,K)^{-1}$	Ager and Howard (1986)
$NaO + CO_2 \rightarrow NaCO_3$	297	$(1{\cdot}3 \pm 0{\cdot}4) \times 10^{-27} (T/200\,K)^{-1}$	Ager and Howard (1986)
$NaOH + CO_2 \rightarrow NaHCO_3$	290	$(1{\cdot}9 \pm 0{\cdot}5) \times 10^{-28} (T/200\,K)^{-1}$	Ager (1986)
$Li + O_2 \rightarrow LiO_2$	267–1100	$(6{\cdot}3 \pm 0{\cdot}6) \times 10^{-30} (T/200\,K)^{-0{\cdot}93}$	Plane and Rajasekhar (1988b)
$K + O_2 \rightarrow KO_2$	250–1103	$(1{\cdot}3 \pm 0{\cdot}2) \times 10^{-29} (T/200\,K)^{-1{\cdot}23}$	Plane *et al.* (1990)
	680–1010	$(1{\cdot}9 \pm 0{\cdot}2) \times 10^{-29} (T/200\,K)^{-1{\cdot}45}$	Husain *et al.* (1987)
	300–700	$(6{\cdot}8 \pm 0{\cdot}3) \times 10^{-30} (T/200\,K)^{-0{\cdot}56}$	Silver *et al.* (1984b)
Remarks: the result of Plane *et al.* (1990) is recommended (see text)			

3. *Photolysis rates*

Reaction	Temperature range of experiment (K)	J (s^{-1})	Reference
$NaCl + h\nu \rightarrow Na + Cl$	300	$(1{\cdot}9 \pm 0{\cdot}8) \times 10^{-4}\ s^{-1}$	Silver *et al.* (1985)
$NaO_2 + h\nu \rightarrow Na + O_2$	230	$(4{\cdot}8 \pm 2{\cdot}9) \times 10^{-3}\ s^{-1}$	Rajasekhar *et al.* (1989)

Table 2. Experimental estimates of rate coefficients for metal reactions of atmospheric interest.

Reaction	Temperature range of experiment (K)	k (cm^3 molecule^{-1} s^{-1})	Reference
$NaO_2 + O \rightarrow NaO + O_2$	300	about 5×10^{-13}	Plane (1989)
$NaOH + H \rightarrow Na + H_2O$	308	$> 4 \times 10^{-12}$	Silver *et al.* (1984a)
$LiOH + H \rightarrow Li + H_2O$	850–1000	$(1{\cdot}2 \pm 0{\cdot}4) \times 10^{-10} \exp(-500\ K/T)$	Plane and Rajasekhar (1988a)
$NaCl + H \rightarrow Na + HCl$	308	about $5 \times 10^{-(14+1)}$	Silver *et al.* (1984a)
	590–820	$k(200\ K) = (1{\cdot}1^{+2{\cdot}3}_{-0{\cdot}8}) \times 10^{-14}$	Plane *et al.* (1989b)

Table 2 contains a list of reactions of atmospheric interest for which the rate coefficient was reported to be approximate or is preliminary data. In view of the uncertainty of these rate constants, they are listed here at the temperature given in the original papers.

3.3. *Summary*

This section has demonstrated that experimental techniques have been successfully developed to study the reactions that metal atoms and metallic species undergo with a variety of reactive atmospheric species, such as O, O_2, O_3, H and HCl. Although the body of kinetic data is far from comprehensive (indeed, the reactions of major meteoric species such as Fe and Mg remain to be studied), in the case of Na a reasonable set of data now exists. In order to understand how these reactions control the chemistry of Na in the upper atmosphere, modelling is required. This is the subject of the next section.

4. Modelling the chemistry of metals in the upper atmosphere

The modelling of an atmospheric phenomenon tends to progress from the simplest zero-dimensional model accounting for the general nature of the phenomenon to models of increasing dimensionality and more detailed chemistry that describe higher-order effects. Indeed, the history of modelling mesospheric metal chemistry began with a qualitative account by Chapman (1939), who used just three reactions to explain the presence of the layer of atomic Na at 90 km and the observed D-line emission in the nightglow. Later models of greater complexity have sought to explain, in an increasingly quantitative fashion, the more detailed features such as the small top and bottom scale-heights of the metal layers, their diurnal and seasonal variability, and the appearance of SSLs.

Three major problems have constrained these efforts. First, the distributions of the free atoms and their ions are known, but observations in the mesosphere have given no information concerning the nature and abundance of the metal compounds. Secondly, since there is no possibility at present of measuring the distribution of the metal compounds, discussion of their chemistry must be based on information from laboratory studies of the pertinent reaction kinetics: only recently has reliable kinetic data started to become available. Thirdly, there has been uncertainty about the sources of the metals in the upper atmosphere, and hence the nature of the metal input flux that is required in a model. This third problem is discussed in section 4.1. The history of modelling mesospheric metal chemistry is then reviewed in section 4.2. In section 4.3 a detailed description is given of a current model developed to include the most recent kinetic studies described in section 3. A sensitivity analysis is then performed on this model in order to identify major uncertainties of the chemistry that should be addressed in future laboratory studies. Section 4.4 contains a description of the chemistry of metallic species in the stratosphere, and their possible impact on the chlorine-catalysed removal of ozone.

4.1. *The sources of metals in the upper atmosphere*

The two sources that have received serious attention are an aerosol or dust layer at about 90 km from which the metals evaporate during the daytime (Hunten and Wallace 1967) and meteoric ablation (Gadsden 1968, 1969, 1970, 1971). One of the general results of early workers was that at altitudes above 90 km the atomic-Na density was

proportional to the total amount of Na (free and bound) at each altitude. This implied, given the steep topside of the Na layer, that the total amount of Na did not have the same scale-height as the other constituents of the atmosphere, a remarkable conclusion in view of the strong turbulent mixing at these altitudes. Hunten and Wallace (1967) postulated that there is a strong source of Na near the peak Na density (i.e. close to 90 km), and a sink higher up. The proposed sink is provided by a layer of dust particles distributed with a scale-height of 3 km, from which Na evaporates copiously during the day owing to heating of the particles or photosputtering by ultraviolet photons. Fiocco *et al.* (1975) have demonstrated that very small particles can reach a radiative-equilibrium temperature in the daytime that is much higher than the ambient atmosphere. Na then condenses back on to the dust at night. Further evidence for this theory was provided by the discovery by Volz and Goody (1962) that, while atmospheric dust has a constant mixing ratio up to 65 km, above 90 km the velocity of fall becomes significant and dust settles in a layer at about 90 km, the topside of this layer showing a similar seasonal variation to the Na layer.

Donahue and Meier (1967) suggested that the source of the dust might be from the Earth's surface (i.e. oceanic or volcanic), or of interplanetary origin. Hunten and Wallace (1967) also proposed that the dust could be formed from the condensation of ablated meteoric material. The observed Na/K ratio in the mesospheric metal layers was used to assess these possibilities. This ratio ranges from about 10 in summer to about 50 in winter (Megie *et al.* 1978). The cosmic Na/K ratio is between 7 and 13, and the same range is typical of minerals in the Earth's crust and the Sun's photosphere (Lytle and Hunten 1959). The ratio in meteoritic material is 13 (Mason 1971). Meanwhile, the seawater ratio is 47·2. Thus Donahue and Meier (1967) hypothesized that the vertical transport of sea-salt particles during storms in the polar night could be responsible for the enhancement of Na over K, which is greatest at high latitudes (section 2). Gadsden (1983) has reported that, after the recent Mount St Helen's eruption, volcanic dust significantly increased the Li abundance in the atmosphere, though such eruptions are of course an irregular occurrence and therefore cannot be the exclusive source of Li.

However, recent observations indicate that dust is probably only a minor source of the gas-phase metals. Firstly, lidar studies have demonstrated the absence of a significant diurnal variation in the Na layer (Granier and Megie 1982): a daytime enhancement in Na would be expected if evaporation from dust were the major source. Secondly, the mesospheric Na/Li ratio remains constant or may even decrease during winter (Jegou *et al.* 1980). This tends to rule out a wintertime source of marine aerosol, although the point should be made that the use of abundance ratios is based on the assumption that the metals have identical chemistries, which we shall see is not quite the case. Thirdly, the small scale-height of the Na layer can be understood by a competition between upward mixing of Na atoms from sources between 80 and 90 km, and photo-ionization at higher levels (see section 4.2). Hunten (1967) has also questioned whether there is sufficient dust above 90 km to provide a fast enough sink for atomic Na to cause the small scale-height of 2–3 km on the topside of the Na layer.

There is, by contrast, very strong evidence that the major source of these metals is meteoric. For instance, there is a good correlation between the relative abundances of ions observed in the mesosphere and the elemental abundances in chondritic meteorites (Goldberg and Aikin 1973, Hermann *et al.* 1978). Figure 18 illustrates such a correlation. In this case, the ions were measured between 91 and 107·5 km. At these altitudes, atomic O is a dominant species that will tend to reduce any molecular ions

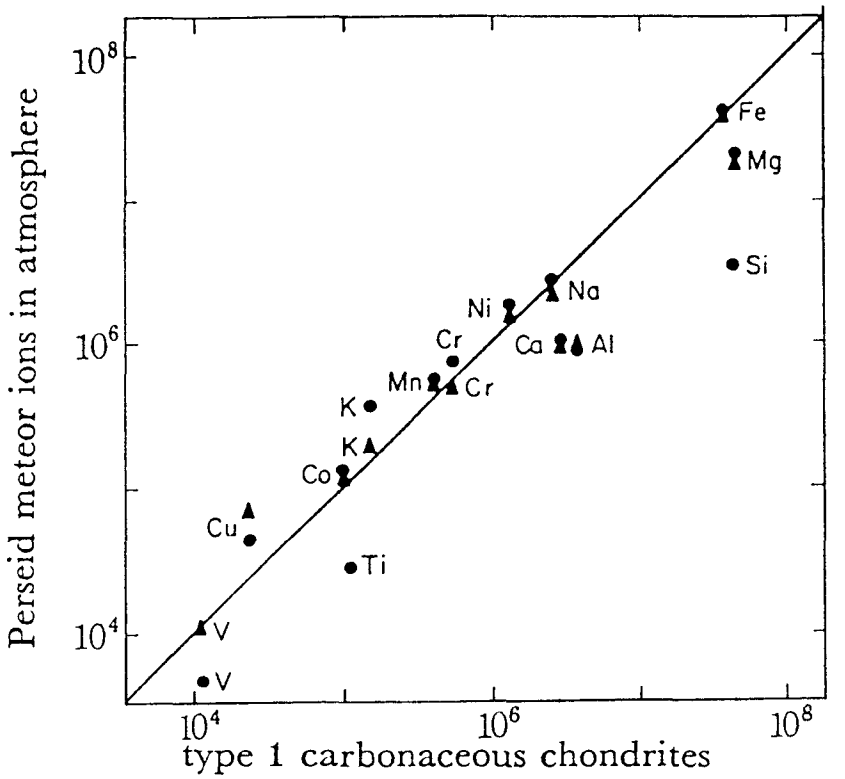

Figure 18. A comparison of the relative concentrations of metal ions observed between 91 and 107·5 km and of metal atoms in carbonaceous chondrites, normalized to the values for iron (Hermann *et al.* 1978): ●, 99–107·5 km; ▲, 91–99 km. (Reproduced from Thomas (1980).)

back to the free metal ions (Ferguson and Fehsenfeld 1968). Hence the metal ions are probably a good measure of the total metal abundance, and so the relative abundance of the ions is a useful quantity. With the exception of Ti and Si, the agreement is rather compelling. Meanwhile, observations that have been linked directly to meteoric showers include sporadic enhancements of the total column abundance of Na (Megie and Blamont 1977, Clemesha *et al.* 1980), short-lived enhancements in the Na nightglow (Kirchhoff and Takahashi 1984), and very short-lived meteor trails (Beatty *et al.* 1988).

Hunten *et al.* (1980) postulated that most of the incoming meteoric mass is in the form of meteoroids in the mass range of 10^{-6}–10^{-3} g (mass median $\approx 10\,\mu g$), with a radius range of 50–500 μm (median radius $\approx 100\,\mu m$). The mean velocity lies between 14·5 and 17 km s^{-1}, so that most of the meteoric material entering the Earth's atmosphere ablates in the 80–100 km region, providing a direct source of metal vapour. In the case of Na, estimates of the average influx of Na from meteoric ablation have been in the range $(1{\cdot}3\text{–}1{\cdot}7) \times 10^4$ cm^2 s^{-1} (Junge *et al.* 1962, Gadsden 1983).

4.2. *The historical development of models of the mesospheric sodium layer*

In the account that follows, chemical reactions are numbered according to the order in which they are given in table 3 (p. 89). This table contains a complete listing of the reaction scheme in the current Na model discussed in section 4.3, where the reactions have been grouped according to the sodium species involved.

Chapman (1939) published the first model of the Na layer, and used the reactions

$$Na + O_3 \rightarrow NaO + O_2, \quad (1)$$

$$NaO + O \rightarrow Na(^2P \text{ and } ^2S) + O_2, \quad (2)$$

$$Na + O + M \rightarrow NaO + M \qquad (M = \text{third body}) \quad (1a)$$

to explain qualitatively the observed nightglow by the formation of $Na(^2P)$ in a cycle with NaO. (Reaction (1 *a*) is no longer considered to be an important atmospheric reaction.) Chapman (1939) proposed that this chemiluminescent cycle involving freshly ablated Na is also responsible for long-endurance visible meteor trials, which can occasionally last for several minutes. Furthermore, this model accounted for the appearance of free atoms at these heights, since it is in the 80–90 km region of the atmosphere that the ratio $[O]:[O_3]$ increases sharply and the atmosphere becomes reducing rather than oxidizing (Wayne 1985).

Later models (Bates 1947, 1954, 1960, Hunten 1954, Omholt 1957, Blamont and Donahue 1964) elaborated on this basic scheme, adding the chemistry of NaO_2:

$$Na + O_2 + M \rightarrow NaO_2 + M, \quad (7)$$

$$NaO_2 + O \rightarrow NaO + O_2. \quad (8)$$

Reaction (7) was studied by seeding Na into oxygen-rich flames and shown to be very slow, $k_7 \approx 10^{-33}$ cm^6 molecule^{-2} s^{-1} (Kaskan 1965, Carabetta and Kaskan 1968). In the absence of measured rate coefficients for any of the other reactions, Blamont and Donahue (1964) set these equal to the analogous reactions of hydrogen atoms or hydrogen oxides, taken from a review by Kaufman (1964). Hunten (1967) later adjusted these rate coefficients to take account of the lower collision frequencies of the Na reactions relative to their H analogues. Unfortunately, recent kinetic studies (section 3) have now shown that this procedure yielded very poor estimates. For example, k_1 was underestimated by a factor of 100, and k_2 by a factor of 10. The poor analogy between H and Na, notwithstanding the fact that they are both ^2S atoms, arises from the much lower ionization energy of Na, which allows it to take part in 'harpoon' or electron-capture reactions (Herschbach 1966). This was pointed out by Kolb and Elgin (1976), who produced a modified Chapman mechanism to explain the Na nightglow and the D-line emission that is observed from meteor trails. They included the additional reaction

$$NaO + O_3 \rightarrow NaO_2 + O_2, \quad (3a)$$

$$\rightarrow Na + 2O_2. \quad (3b)$$

Kolb and Elgin (1976) estimated the rate coefficients of reactions (1), (2) and (3) by calculating reaction cross-sections using the electron-capture mechanism. This procedure gave rate coefficients that turned out to agree well with the subsequently measured values (table 1).

Mass-spectrometric measurements of positive ions in the stratosphere (Arnold *et al.* 1977, 1978) have indicated the presence of a series of complex cluster ions, which Ferguson (1978) interpreted as being NaOH clusters of the form $NaOH_2^+(NaOH)_m(H_2O)_n$. This was evidence that NaOH is an important Na species in the upper atmosphere, and Liu and Reid (1979) included the following reactions in a model of Na chemistry:

$$NaO_2 + H \rightarrow NaOH + O, \quad (9)$$

$$NaOH + H \rightarrow Na + H_2O, \tag{11}$$

$$NaOH + h\nu \rightarrow Na + OH \tag{12}$$

as well as other reactions involving OH and HO_2 that are probably of secondary importance.

Husain and Plane (1982a) showed, using the flash-photolysis/time-resolved resonance-absorption technique, that k_7 was actually about 10^3 times greater than the flame study of Carabetta and Kaskan (1968) had indicated. Hence NaO_2 is very likely to be a major Na species below 90 km (Sze *et al.* 1982, Thomas *et al.* 1983, Plane 1984, Swider 1985, 1986, 1987). Swider (1985, 1986) showed recently that a basic scheme involving reactions (1), (2), (7) and (8) can account for most of the important features of the Na layer below 95 km. He demonstrated that reaction (7) is important for controlling the seasonal variation in the column density of atomic Na. This is because the rate of reaction (7) has an *overall* temperature dependence of about $T^{-3.2}$. This arises first from the $T^{-1.2}$ dependence of k_7 (Plane and Rajasekhar 1989). The reaction rate is also proportional to $[O_2]$ and to [M], and hence to $[M]^2$, because $[O_2] = 0.21$ [M] below 95 km (Wayne 1985), and [M] is approximately proportional to T^{-1}. Hence the ability of reaction (7) to convert Na to NaO_2 *increases* rapidly at lower temperatures. Furthermore, a preliminary measurement by Plane (1989) has shown that reaction (8), which effectively returns NaO_2 to Na, is slow and hence probably has a significant activation energy (table 2). Its rate will thus *decrease* at lower temperatures, further enhancing the conversion of Na to NaO_2. Swider (1986) has also shown that the intensity of the Na D-line emission in the nightglow is somewhat decoupled from the Na column density, as observed (section 2.2). This is because reactions (1) and (2) constitute a rapid catalytic cycle that does not remove atomic Na. Hence fluctuations in the O_3 density will have a directly proportional effect on the nightglow intensity, but will have a small impact on the Na column density. Swider (1987) has also developed an analogous model of the K layer, postulating that the lack of a seasonal variation in the K column density (section 2.2) may be explained by the reaction $KO_2 + O$ having a smaller activation energy than that of reaction (8).

There was much discussion up to the 1970s concerning the role of Na^+ ions as a reservoir for Na (Bates 1947, Omholt 1957, Sullivan and Hunten 1964, Gadsden 1964, Donahue 1966). At that time, only the rate of photo-ionization

$$Na + h\nu \rightarrow Na^+ + e \tag{14}$$

was known (Hunten 1967). Ferguson (1978) subsequently showed that the rates of the charge-transfer reactions

$$Na + O_2^+ \rightarrow Na^+ + O_2 \tag{15}$$

$$Na + NO^+ \rightarrow Na^+ + NO \tag{16}$$

are sufficiently high that these processes, at the ambient levels of NO^+ and O_2^+ ions in the mesosphere, compete with photo-ionization as sources of Na^+.

The rocket flights reported by Narcisi (1966) showed that the Na^+ column density was about 10% that of the neutral Na atoms. This degree of ionization is too small to affect significantly the behaviour of the neutral layer as a whole, although Hanson and Donaldson (1967) have proposed that the ionization of Na atoms is responsible for the small scale-height on the top side of the Na layer.

The lack of ionization indicates that an efficient mechanism must exist to convert Na^+ back to Na. The rate of direct recombination between Na^+ and an electron is negligible (Smith 1980, Wayne 1985). A more likely route is through dissociative recombination between a molecular Na ion and an electron (Brown 1973). Ferguson and Fehsenfeld (1968) showed in the laboratory that Na^+ (and K^+) do not appear to react with either O_3 or O_2 to give the metal oxide or superoxide ions respectively. Instead, Richter and Sechrist (1979) considered the clustering of Na^+ ions to CO_2 and N_2 molecules as intermediate stages in the hydration of the metal ions, by direct analogy with the corresponding processes for NO^+ ions in the D-region (McEwan and Phillips 1975). Thus

$$Na^+ + N_2 + M \rightarrow Na^+ . N_2 + M \tag{17}$$

is followed by a series of switching reactions to form more stable ion clusters:

$$Na^+ . N_2 + CO_2 \rightarrow Na^+ . CO_2 + N_2, \tag{17a}$$

$$Na^+ . CO_2 + H_2O \rightarrow Na^+ . H_2O + CO_2. \tag{17b}$$

Any of these ion clusters will undergo a dissociative recombination reaction with an electron to yield back Na:

$$Na^+ . X + e \rightarrow Na + X \qquad (X = N_2,\ CO_2 \text{ or } H_2O). \tag{18}$$

This ion chemistry was incorporated into the model of Thomas *et al.* (1983) to describe the Na chemistry on the top side of the neutral layer.

Photochemical models of Na in the mesosphere must support the downward flux from meteoric ablation at the top of the layer by providing a permanent sink below 80 km. Following the demonstration that ionization is not an effective reservoir for Na, three other sinks have been considered: deposition on dust particles (Hunten 1981), the formation of hydrated cluster ions (Jegou *et al.* 1985) and the formation of stable Na compounds in the gas-phase such as NaOH and NaO_2 (Liu and Reid 1979, Kirchhoff *et al.* 1981, Sze *et al.* 1982, Thomas *et al.* 1983, Plane 1984, Swider 1985, 1986, 1987). Hunten *et al.* (1980) calculated a height profile of meteoric ablation. By including the flux of micrometeorites and residual meteoroids, and also considering the coagulation of evaporated silicates into 'smoke' particles, they estimated a total particle surface area of close to $10^{-9}\,cm^2\,cm^{-3}$ below 90 km. Combining this surface area with a collision frequency per unit area of about $10^4\,cm\,s^{-1}$, and assuming an accommodation coefficient of unity for all neutral and ionic Na species, the rate of first-order loss for these species on to dust particles is about $10^{-5}\,s^{-1}$ (Hunten 1981). If thermal evaporation of Na from these particles is ignored, Hunten (1981) found that almost all the Na species will then reside on dust below 80 km. This result depends on the total particle surface area calculated by Hunten *et al.* (1980), and so the importance of this mechanism as a sink for Na species remains uncertain in the absence of actual measurements of the concentration and size distribution of these dust particles. Hunten *et al.* (1980) showed that the dust is undetectable by optical methods, and confirmation from balloon studies of condensation nuclei in the stratosphere remains indirect and rather variable. The importance of this mechanism might be demonstrated if future laboratory studies were to indicate that the gas-phase Na compounds are not sufficiently stable in the mesosphere, so that an additional sink is required. Hunten (1981) also postulated that the large winter enhancement of atomic Na at high latitudes could be explained by the much lower rate of ionization over the polar cap during

winter, and that the different seasonal behaviour of K was due to an additional sink provided by Penning ionization with metastable O_2. These hypotheses depend on the metallic ions being permanent sinks, in this case through deposition on to dust particles. Note, however, that reactions (17) and (18) may provide an efficient mechanism for cycling the ions back to the neutral atoms.

Jegou *et al.* (1985) have recently put forward a model in which the neutral-atom chemistry around 90 km is controlled by the dynamics of hydrated metal-ion clusters, whose source is meteoric ablation at about the 100 km level. A theoretical treatment to explain the layering and the downward flux of these ion clusters has been proposed by Chimonas and Axford (1968). In the E region of the upper atmosphere, the frequencies with which the ions gyrate around the geomagnetic field lines and the frequencies with which they undergo collisions with neutral particles are comparable. Under these circumstances, a horizontal East–West wind causes both horizontal transport and a vertical Lorentz force to operate on the ions. In the case of a wind directed toward the East in the Northern hemisphere, an upward movement is imposed on ions, whereas a wind towards the West imposes a downward movement; a convergence is then effected at a height of suitable wind shear. Chimonas and Axford (1968) proposed that the metal ions will remain at the nulls of the wind pattern in the case of a periodic wind structure that has a downward phase velocity. This will persist until the collision frequencies are too high to permit the downward movement of the layer to continue and it is dispersed by diffusion, probably in the 80–90 km region.

Rowlett *et al.* (1978) have observed with lidar a wave-like structure in the neutral Na layer, with about a 4–10 km wavelength and a downward motion of $0{\cdot}5\,m\,s^{-1}$. This downward motion is quite close to the value suggested for the downward motion of layered ions by Chimonas and Axford (1968), and Rowlett *et al.* (1978) considered that the free Na atoms may be serving as a tracer to enable this effect to be monitored. Jegou *et al.* (1985) suggested that these ions are converted to NaOH at about 70 km, and this provides a permanent sink. They also presented a detailed scheme of the ion-clustering reactions of Na^+, K^+ and Li^+. By postulating temperature-dependent differences in the ion-cluster chemistries of these ions, they argued that the different seasonal behaviour of the three neutral metal atoms could be explained. However, this theory remains a matter of conjecture in the absence of laboratory confirmation of the proposed cluster chemistry.

As we shall see in section 4.3, current models of Na chemistry that employ the revised value of k_7 (table 1) are able to account for most of the observed features of the Na layer (Sze *et al.* 1982, Thomas *et al.* 1983, Plane 1984, Swider 1985, 1986, 1987). The rate of this termolecular reaction is proportional to both O_2 and the total pressure: since O_2 is also proportional to the total pressure, the rate of reaction (7) will increase with the *square* of the atmospheric pressure. Hence the rate at which this reaction removes Na has a negative scale-height equal to half that of the atmosphere, and this accounts for most of the small scale-height on the underside of the Na layer (section 2.2).

4.3. *A current model of mesospheric sodium chemistry*

The model that is presented here has been adapted from that of Thomas *et al.* (1983) by including the results of recent laboratory studies. It is a one-dimensional dynamical model involving both photochemistry and ionization, solved over an altitude range of 65–110 km for conditions of the atmosphere at noon and at midnight, in order to test for diurnal variations in the Na-layer structure. Account is taken of the eddy-diffusion

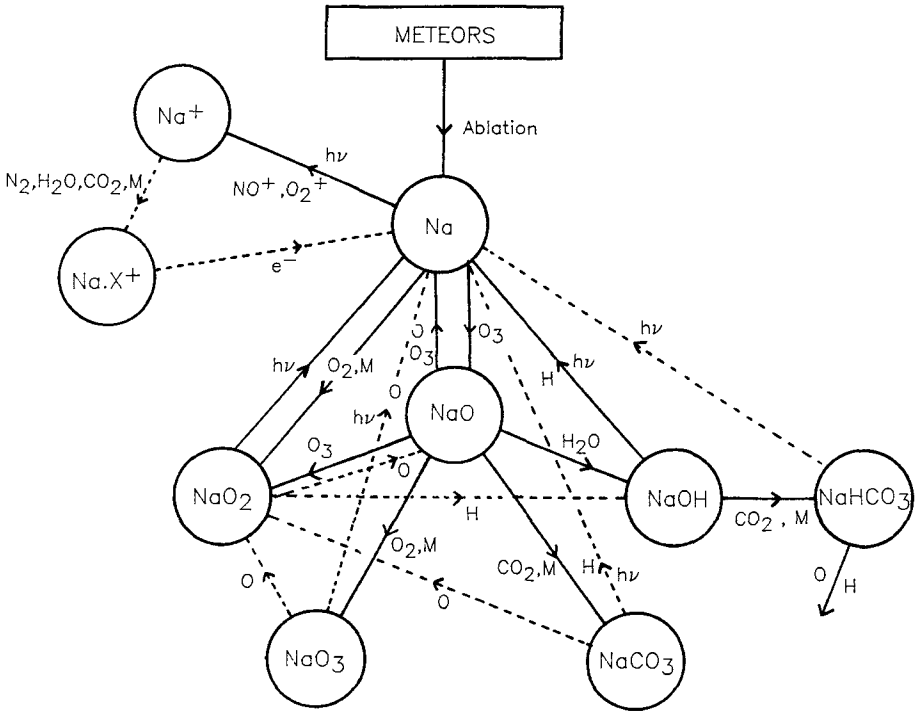

Figure 19. A schematic diagram of the gas-phase chemistry of sodium in the mesosphere in the model in section 4.3. Solid lines indicate reaction pathways for which absolute rate coefficients have been measured in the laboratory. Broken lines indicate pathways that have been postulated in models.

coefficient up to the turbopause (105 km), above which molecular diffusion is assumed. Transport of electrodynamical origin is neglected. Estimates of the daytime and nighttime profiles of the ambient minor atmospheric constituents O_3, O and H are taken from Thomas *et al.* (1983). Estimates of the O_2^+, NO^+ and electron concentrations given by Narcisi (1973) for the daytime have been used.

Figure 19 is a diagram that summarizes the gas-phase chemistry of Na in the mesosphere included in the present model. The model assumes that atomic Na is injected into the atmosphere through meteoric ablation, and then transformed into NaO, NaO_2, NaOH, NaO_3, $NaCO_3$, $NaHCO_3$, Na^+ and assorted ion clusters. The assumption is also made that equilibrium is maintained by a downward flux of Na constituents equal to the meteoric influx, and that this flux is finally lost in a lower-atmospheric sink. This could be provided by eventual rain-out into the troposphere, or incorporation into aerosols such as the Junge layer (Junge and Manson 1961), where the individual particles are known to contain most of the meteoric metals (Shedlovsky and Paisley 1966, Lazrus and Grandrud 1971, Cadle 1972, Delaney *et al.* 1974).

4.3.1. *Model reaction scheme*

Table 3 is a complete list of the reactions currently in the model. The table is divided into three sections: neutral, ionic and closure reactions. The set of closure reactions is required to achieve model closure when the distribution of the total Na content among the various Na constituents is calculated at each altitude in the model. The closure

Table 3. The reaction scheme in a current model of Na species in the mesosphere.

Reaction	Rate coefficient (200 K)†	Reference
Neutral reactions		
(1) $Na+O_3 \rightarrow NaO+O_2$	$6{\cdot}0\times10^{-10}$	Husain *et al.* (1985b) Silver and Kolb (1986) Ager *et al.* (1986)
(2) $NaO+O \rightarrow Na(^2P,^2S)+O_2$	$2{\cdot}2\times10^{-10}$	Plane and Husain (1986)
(3*a*) $NaO+O_3 \rightarrow NaO_2+O_2$	$1{\cdot}5\times10^{-10}$	Ager *et al.* (1986)
(3*b*) $\rightarrow Na+2O_2$	$2{\cdot}0\times10^{-11}$	
(4) $NaO+H_2O \rightarrow NaOH+OH$	$1{\cdot}8\times10^{-10}$	Ager and Howard (1987)
(5) $NaO+O_2+N_2 \rightarrow NaO_3+N_2$	$5{\cdot}3\times10^{-30}$	Ager and Howard (1986)
(6) $NaO+CO_2+N_2 \rightarrow NaCO_3+N_2$	$1{\cdot}3\times10^{-27}$	Ager and Howard (1986)
(7) $Na+O_2+N_2 \rightarrow NaO_2+N_2$	$4{\cdot}7\times10^{-30}$	Plane and Rajasekhar (1989) Husain *et al.* (1986) Silver *et al.* (1984b)
(8) $NaO_2+O \rightarrow NaO+O_2$	2×10^{-14}	Estimate
(9) $NaO_2+H \rightarrow NaOH+O$	$1{\cdot}9\times10^{-14}$	Estimate
(10) $NaO_2+h\nu \rightarrow Na+O_2$	$4{\cdot}8\times10^{-3}$	Rajasekhar *et al.* (1989)
(11) $NaOH+H \rightarrow Na+H_2O$	4×10^{-13}	Estimate
(12) $NaOH+h\nu \rightarrow Na+OH$	1×10^{-3}	Estimate
(13) $NaOH+CO_2+N_2 \rightarrow NaHCO_3+N_2$	$1{\cdot}9\times10^{-28}$	Ager (1986)
Ionic chemistry		
(14) $Na+h\nu \rightarrow Na^+ + e$	2×10^{-5}	Kvifte (1973)
(15) $Na+O_2^+ \rightarrow Na^+ + O_2$	$1{\cdot}4\times10^{-9}$	Ferguson and Fehsenfeld (1968)
(16) $Na+NO^+ \rightarrow Na^+ + NO$	1×10^{-9}	Ferguson and Fehsenfeld (1968)
(17) $Na^+ + N_2 + N_2 \rightarrow Na^+.N_2 + N_2$	$2{\cdot}5\times10^{-31}$	Richter and Sechrist (1979)
(18) $Na^+.X(\text{cluster})+e \rightarrow Na+\ldots$	10^{-6}	Estimate
Closure reactions		
(19) $NaO_3+O \rightarrow Na+2O_2$	2×10^{-14}	Estimate
$\rightarrow NaO_2+O_2$	2×10^{-14}	
(20) $NaCO_3+O \rightarrow NaO_2+CO_2$	1×10^{-13}	Estimate
(21) $NaCO_3+H+N_2 \rightarrow NaHCO_3$	1×10^{-30}	Estimate
(22) $NaHCO_3+H \rightarrow Na+H_2CO_3$	1×10^{-14}	Estimate
(23) $NaHCO_3+h\nu \rightarrow Na+HOCO_2$	2×10^{-4}	Estimate

† *Units*: unimolecular reaction in s^{-1}; bimolecular in $cm^3\,molecule^{-1}\,s^{-1}$; and termolecular in $cm^6\,molecule^{-2}\,s^{-1}$.

reactions are at present hypothetical. They are exothermic reactions between NaO_3, $NaCO_3$ or $NaHCO_3$ and reactive atmospheric radicals such as O and H, and have been assigned relatively slow rate coefficients whose values do not significantly affect the neutral Na layer, but rather affect the partitioning of Na between these various constituents below 80 km.

Each reaction in table 3 has been assigned a rate coefficient at 200 K, which is also listed in the table along with a reference to the source. In the case of reactions that have been studied experimentally, the extrapolated values of the rate coefficients are derived from the expressions in table 1. Several of the neutral reactions have had to be given estimated rate coefficients. k_8 is chosen to be a sensible extrapolation of the preliminary room-temperature value in table 2. k_9 and k_{11} are taken from the model of Thomas *et al.* (1983). In fact, reaction (11) has been studied at high temperatures in flames by Jensen and Jones (1982). Their extrapolated rate coefficient yields

$k_{11}(200\,\mathrm{K}) \approx 10^{-13}\,\mathrm{cm^3\,molecule^{-1}\,s^{-1}}$. This value is also in accord with the room-temperature lower limit in table 3. The rate of reaction (12), the photolysis of NaOH, has been estimated by Rowland and Makide (1982) to be $J(\mathrm{NaOH}) = 6 \times 10^{-2}\,\mathrm{s^{-1}}$. However, we have found that, combined with the measured photolysis rate for NaO_2 (Rajasekhar *et al.* 1989), this value for J(NaOH) yields too large a diurnal variation in Na density. Since J(NaOH) was derived from measurements in flames (Rowland and Makide 1982) where the NaOH is highly vibrationally excited, the value is probably considerably overestimated. Reaction (17) is an equivalent reaction representing the initial clustering between Na^+ and N_2 followed by switching with CO_2 and H_2O to form assorted Na ion clusters, termed here $Na^+ . X$. Reaction (18) is assigned a rate coefficient based on laboratory measurements for the dissociative recombination of hydrated protons with electrons (Leu *et al.* 1973).

4.3.2. *The total sodium profile*

Turbulent mixing, expressed by the eddy-diffusion coefficient, is more important than molecular diffusion in describing transport processes in the atmosphere below the turbopause at about 105 km. Since the motion of all atmospheric constituents is then governed by the same eddy-diffusion coefficient, it is possible to describe the height variation of the total concentration of a particular element without reference to the chemical lifetimes of the various molecules that contain that element (Thomas 1974). It can then be shown (Thomas 1974), if n(Na) is the total number density of Na summed over all Na-containing molecules at height z, that

$$n(\mathrm{Na}) = \underline{n(\mathrm{Na})}\left[1 - \Phi(\mathrm{Na}) \int_{z_0}^{z} \frac{\mathrm{d}z'}{K\underline{n(\mathrm{Na})}}\right], \tag{4.1}$$

where Φ(Na) is the total sodium flux summed over all Na species, K is the eddy diffusion coefficient, and $\underline{n(\mathrm{Na})}$ is the solution for $\Phi(\mathrm{Na}) = 0$ (i.e. for the case where the total Na density has the same scale-height as the general atmosphere). This treatment ignores thermal diffusion in the mesosphere and also assumes that each Na species contains only one Na atom. The scale-height of the total Na density must in fact be greater than that of the general atmosphere in order to support the downward flux. Equation (4.1) is solved by numerical integration to yield the total Na density profile. The value of $\underline{n(\mathrm{Na})}$ at 65 km ($= z_0$) is an adjustable parameter, which is chosen to yield a value for the free Na column density in the observed range $(4\text{–}5) \times 10^9\,\mathrm{cm^{-2}}$ (see section 2.2). Values of the eddy-diffusion coefficient K are taken from Thomas and Bowman (1972). The mean value is about $10^6\,\mathrm{cm^2\,s^{-1}}$. The value of the total Na influx from meteoric ablation has been set equal to $1{\cdot}3 \times 10^4\,\mathrm{cm^{-2}\,s^{-1}}$ (Gadsden 1983), and the ablation is assumed to follow the profile of Hunten *et al.* (1980).

4.3.3. *Model calculations*

The model considers that there are nine Na species coupled in a steady-state through the reactions in table 3. The density profiles for the species are then calculated at 0·5 km intervals by solving the total-density equation

$$\begin{aligned} n(\mathrm{Na}) = {} & [\mathrm{Na}] + [\mathrm{NaO}] + [\mathrm{NaO_2}] \\ & + [\mathrm{NaOH}] + [\mathrm{NaO_3}] + [\mathrm{NaCO_3}] \\ & + [\mathrm{NaHCO_3}] + [\mathrm{Na^+}] + [\mathrm{Na^+ . X}] \end{aligned} \tag{4.2}$$

simultaneously with the steady-state relationships coupling the Na species. This treatment assumes that the chemical lifetimes of each species are a few hours at most, which is the case below 95 km. There is also the inherent assumption that the ambient concentrations of O_3, O and H are unaffected by the Na chemistry, which is reasonable since over most of this region they are in excess over the Na species by at least three orders of magnitude, with the exception of the nighttime atomic O concentration below 70 km (Shimazaki 1985).

4.3.4. *Model results*

Figure 20 illustrates modelled profiles of the major Na species for noon and midnight. The NaO_3 and $Na^+ . X$ concentrations are negligible and are not shown. The atomic-Na profiles are seen to correspond loosely to a Gaussian shape in accord with

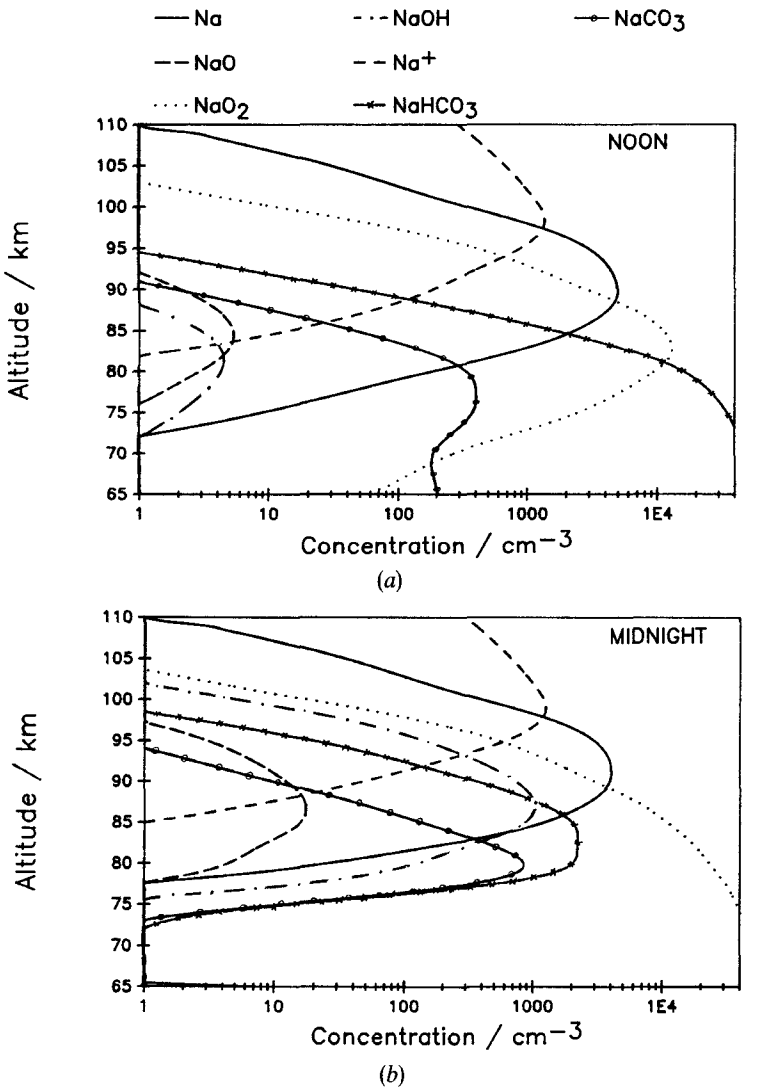

Figure 20. Modelled concentration profiles of the major sodium constituents in the mesosphere under (*a*) daytime and (*b*) nighttime conditions.

observation (Megie and Blamont 1977). The Na-layer peak is at 91 km in both profiles. The peak densities range from $4{\cdot}7 \times 10^3$ to $4{\cdot}1 \times 10^3$ cm^{-3}, and the column densities from $4{\cdot}5 \times 10^9$ to $4{\cdot}3 \times 10^9$ cm^{-2}, for noon and midnight respectively. Thus there are no significant diurnal variations in these parameters, in agreement with recent observations (section 2.2). However, there is a diurnal variation on the underside of the layer below 80 km. This causes the centroid of the layer to move from 90 km during the day to 92 km at night, consistent with the lidar observations of Clemesha *et al.* (1982). Note also the small average scale-height of 2·4 km on the topside of the layer, again in agreement with observation (Sandford and Gibson 1970).

Figure 20 illustrates that NaO_2 is the major species immediately below the peak of the free-Na layer, especially at night. During the day, it is photolysed readily (reaction (10)), and this is mostly responsible for the daytime enhancement of the Na layer below 80 km. Although $NaHCO_3$ appears in the modelling output as the daytime sink below 80 km, this is largely a function of the choice of the closure reactions in table 3. With the cessation of photodissociation after sunset, a significant amount of NaOH can build up through reaction (9), as shown in figure 20. Below 75 km, reaction (13) dominates the removal of NaOH at all times. The sink for Na above 90 km is caused by ionization to Na^+, which becomes the major Na species above 95 km. At night, the observed NO^+, O_2^+ and electron densities decrease by about a factor of 10. If this effect is included in the model, a small increase in Na above 95 km is predicted (Thomas *et al.* 1983). The Na^+ cluster concentration remains negligible because of the extremely fast dissociative recombination reaction with electrons (reaction (18)).

The D-line nightglow profile can be estimated from the original mechanism of Chapman (1939), by integrating the rate of emission over the layer:

$$\phi(589\text{ nm}) = \int \gamma[\text{Na}][\text{O}_3]\,\text{d}z \qquad (4.3)$$

This requires an estimate for the branching ratio γ of reaction (2) to form Na(^{2}P) atoms, which then emit to Na(^{2}S), producing the nightglow lines at 589 nm. Bates and Ojha (1980) have shown that γ can be as high as $\frac{1}{3}$, by correlating the product and reactant states and assuming that an electron-jump mechanism operates. Plane and Husain (1986) estimated γ experimentally, obtaining an upper limit of 1%. This value was obtained in an experiment where the degree of photolysis of NaO by a flash lamp had to be estimated. The recent work of Plane and Nien (1990), which investigated the photolysis of CaO under better characterized conditions with an excimer laser, indicates that the degree of photolysis of NaO may have been overestimated in the earlier study: hence the γ value was probably underestimated.

The present model may be used to compute the nightglow profile, assuming a γ value of $\frac{1}{3}$. This yields an emission layer with a peak at 89·5 km, and a f.w.h.m. of 8·5 km, in good agreement with direct measurements of the Na nightglow using a rocket-borne photometer (Greer and Best 1967), which revealed a layer having a peak emission at 89 km and a f.w.h.m. of 8 km. The integrated intensity from the present model is 106 R, well within the range of between 50 and 200 R from a variety of ground-based observations (Kvifte 1973).

Finally, the temperature dependence of the model can be used to examine whether the neutral chemistry of Na can account for the observed winter enhancement of the layer. The temperature dependences of the rate coefficients in the model are taken from table 1, and the total pressure is set to be inversely proportional to the temperature. The concentrations of minor atmospheric constituents are kept constant. Swider (1985) has

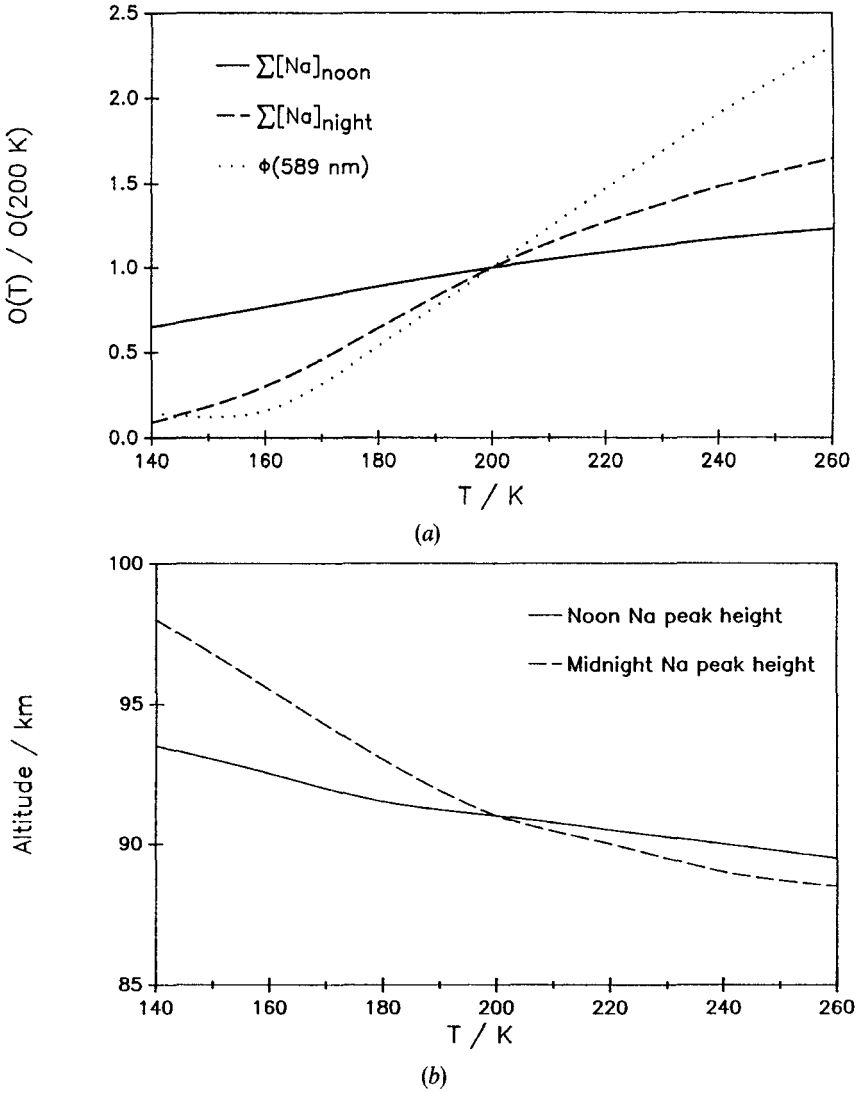

Figure 21. The calculated effect of temperature variations on the mesospheric Na layer: (*a*) the effect on the daytime and nighttime column densities and the D-line nightglow emission, plotted as a ratio of that quantity to its value at 200 K, the reference temperature of the model; (*b*) the effect on the daytime and night-time peak heights of the Na layer.

demonstrated that seasonal changes in mesospheric O-atom concentrations have a relatively small impact on atomic Na. The photolysis rates of the Na species are also kept constant for his calculation. Figure 21 illustrates the effect on the model of varying the temperature. The calculated daytime and nighttime column densities and the nightglow emission all show a large positive temperature dependence, which can account for the approximately threefold increases (section 2.2) that are observed when the mesopause warms from about 140 K in summer to about 210 K in winter (CIRA 1972). Furthermore, the predicted peak height of the layer becomes lower at warmer temperatures, again in accord with observation (Megie *et al.* 1978).

4.3.5. *Sensitivity tests*

The current model of mesospheric Na described above clearly accounts very well for the observed average features of the Na layer.

It should be borne in mind that this model contains a number of poorly known and fitted parameters. This confers a measure of ambiguity on the model, so that the evident success achieved in reproducing the observables does not necessarily constitute a stringent test of the model. The purpose of this section is to apply sensitivity tests in order to ascertain which of these unknown parameters are important. This procedure both reduces the existing ambiguity in the model and indicates where future studies need to be made.

The unknown parameters may be grouped into those quantities that determine the total Na density, and the rate coefficients and photolysis rates which determine the partitioning between the different Na constituents. The observable features against which the model can be tested include the daytime and nighttime column densities, peak heights and peak number densities, the emission intensity, peak height and f.w.h.m. of the nightglow layer, and the seasonal dependences of these parameters. The calculated f.w.h.m. of the nightglow layer turns out to be rather insensitive and is not a good criterion. Also, the calculated *absolute* column and peak number densities and the nightglow emission intensity are clearly functions of the total Na profile, as well as the chemistry. In order to focus on the uncertainties in the chemistry, the *ratio* of the daytime to nighttime column abundances is a better test (to a very good approximation, the Na peak number density and the column density turn out to be proportional because of the Gaussian shape of the Na profile, so that additional consideration of the peak number density is redundant). The peak height of the Na layer is also a good test of the chemistry, because it is not sensitive to the first group of parameters such as the total meteoric influx and the vertical profile of the eddy-diffusion coefficient (Thomas *et al.* 1983): modest changes in these parameters tend only to scale the total Na profile and hence the individual constituents, independent of altitude.

Sensitivity tests, using the criteria of the calculated diurnal variation in column density or the peak height of the Na layer, indicate that the reactions of NaO_2 with H and O (reactions (8) and (9)), and the photolysis of NaOH (reaction (12)) are important unknowns in the current model. Other unknowns, such as the hypothetical chemistry described by the closure reactions in table 3, largely affect the Na chemistry below 80 km, where there are no observables to test against. The results of these sensitivity tests are illustrated in figures 22 and 23. Figure 22 indicates that the value of k_8 cannot be much less than the current value in the model of 2×10^{-14} cm^3 molecule^{-1} s^{-1}. Otherwise, NaO_2 becomes an even more important sink for Na, increasing the peak height of the Na layer to above the observed upper limit of 92 km. Also, because NaO_2 is readily photolysed in the daytime, a diurnal variation in column density becomes apparent, whereas observations show that there is no significant diurnal variation. On the other hand, making k_8 greater than the current value has no effect on either criterion. Hence a lower limit to k_8 appears to be about 9×10^{-15} cm^3 molecule^{-1} s^{-1} at 200 K. The sensitivity of the model to reaction (8) has been noted previously (Thomas *et al.* 1983). Reaction (9) appears to have little effect on the diurnal variation in column density. However, increasing it by a factor of about 30 raises the daytime peak height above 92 km.

Figure 23 illustrates the sensitivity of the model to the photolysis rates of NaOH and NaO_2 (reactions (10) and (12)). Although the photolysis cross-sections of NaO_2

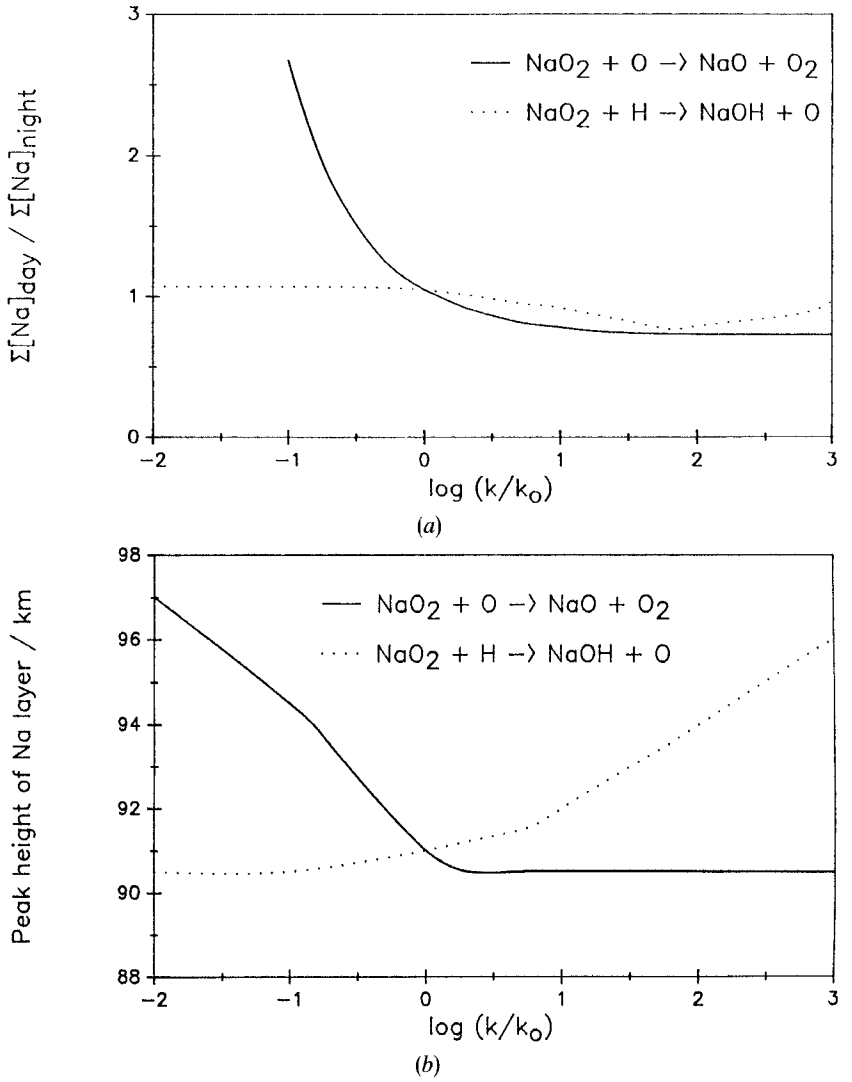

Figure 22. Sensitivity tests of the current model of mesospheric Na. The sensitivity of (*a*) the ratio of the day/night column densities and (*b*) the daytime peak height of the Na layer, are tested against the rate coefficients of the reactions $NaO_2 + O$ and $NaO_2 + H$. The abscissa in each diagram is the logarithm (to base 10) of the ratio of the rate coefficient k to its optimized value k_0 given in table 3.

have been measured at three discrete wavelengths by Rajasekhar *et al.* (1989), the computed photolysis rate is rather uncertain (table 1). The model is sensitive to both $J(NaO_2)$ and $J(NaOH)$. As expected, the diurnal variation in column density increases and the daytime peak height decreases when either of these rates is increased, and *vice versa*. Either rate can be changed independently within a factor of about five without the calculated criteria exceeding the observed values. Laboratory studies of k_8, k_9 and $J(NaOH)$ are clearly a priority. Their measurement would constitute an important test of the predicted partitioning of Na into NaO_2 and NaOH between 80 and 90 km, and of the ability of the neutral chemistry to provide a daytime reservoir for Na.

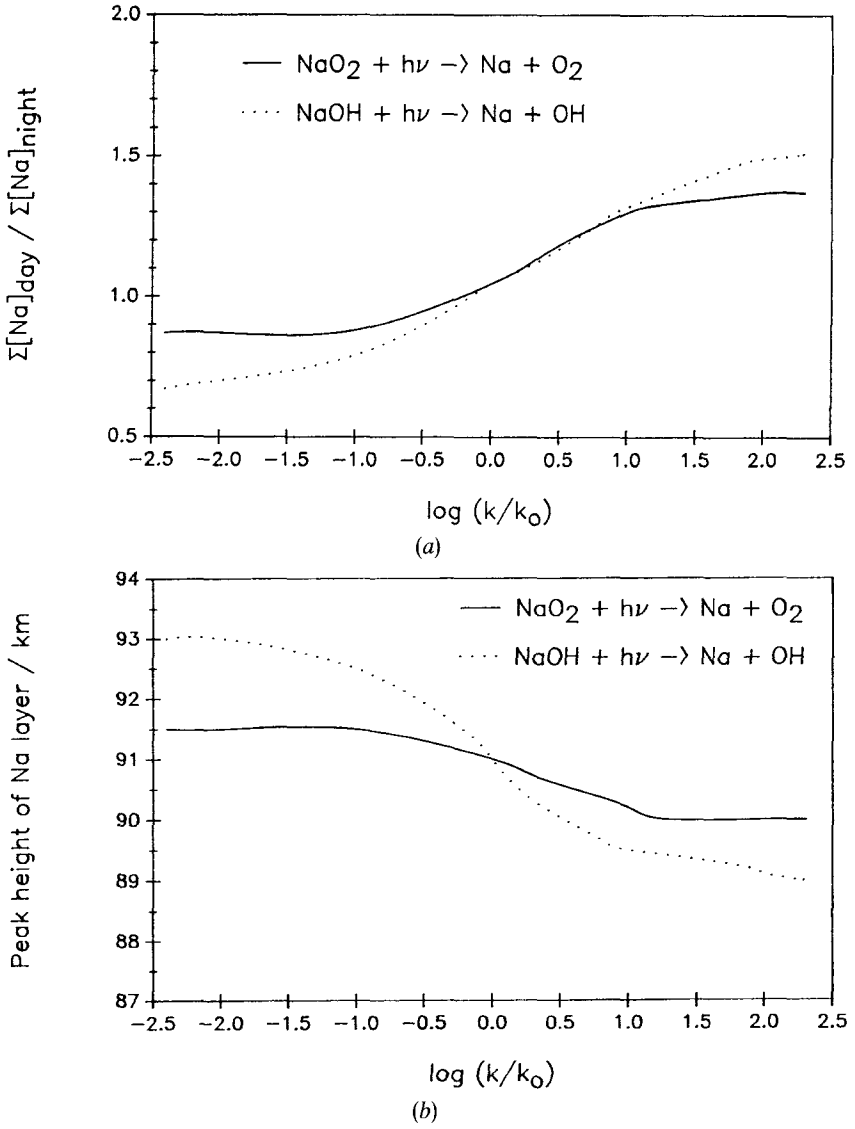

Figure 23. Sensitivity tests of the current model of mesospheric Na. The sensitivity of (*a*) the ratio of the day/night column densities, and (*b*) the daytime peak height of the Na layer, are tested against the photolysis rates of the reactions $NaO_2 + h\nu$ and $NaOH + h\nu$. The abscissa in each diagram is the logarithm (to base 10) of the ratio of the photolysis rate k to its optimized value k_0 given in table 3.

4.4. *Models of the chemistry of meteoric metals in the stratosphere*

The fate of meteoric metals below 80 km is uncertain. As mentioned in section 4.1, there is evidence (Arnold *et al.* 1977, 1978, Ferguson 1978) of the presence of NaOH clusters of the form $NaOH_2^+(NaOH)_m(H_2O)_n$ in the stratosphere. Meanwhile, meteoric metals have been reported in aerosols collected in the lower stratosphere (Shedlovsky and Paisley 1966, Delaney *et al.* 1974, Lazrus and Grandrud 1971) and the troposphere (Cadle and Grams 1975, Charlson *et al.* 1978, Penkett *et al.* 1979, Parungo *et al.* 1979), where they exist as metal chlorides and sulphates.

Recent interest in the chemistry of meteoric metals in the stratosphere has focused on their interaction with stratospheric ozone. Liu and Reid (1979) first suggested that meteoric species might be involved in catalytic reactions such as

$$Fe + O_3 \rightarrow FeO + O_2, \qquad FeO + O \rightarrow Fe + O_2.$$

They estimated from a meteoric-ablation model that the total Na number density at 40 km is nearly $10^6\,cm^{-3}$, or about $10^7\,cm^{-3}$ for all meteoric species, concluding that these concentrations were large enough to warrant inclusion in detailed photochemical models. However, following the demonstration from laboratory kinetic studies (table 1) that the recombination reactions between at least the alkali metal atoms and O_2 to form the superoxides are very rapid, the concentration of free metal atoms in the stratosphere is probably negligible and this mechanism is rather unlikely.

The impact of meteoric species on the chlorine-catalysed removal of ozone is a more serious possibility. The chlorine cycle is most effective in the stratosphere between 40 and 50 km, where it probably accounts for about 30% of total ozone loss (Wayne 1985). Hence this is the part of the atmosphere where perturbations caused by anthropogenic chlorine will be largest. The catalytic efficiency of chlorine compounds in removing stratospheric O_3 is particularly sensitive to the abundance of the active chlorine species Cl and ClO. Chlorine is largely partitioned between these active species and the reservoir species HCl. This partitioning is primarily determined by the following chemistry (Rodriguez *et al.* 1986):

$$OH + HCl \rightarrow H_2O + Cl,$$

$$Cl + CH_4 \rightarrow HCl + CH_3,$$

$$Cl + HO_2 \rightarrow HCl + O_2.$$

Murad *et al.* (1981) argued on a thermochemical basis that Na species such as NaOH and $NaHCO_3$ in the stratosphere would react with HCl to form NaCl:

$$NaOH + HCl \rightarrow NaCl + H_2O,$$

$$NaHCO_3 + HCl \rightarrow NaCl + (H_2CO_3 \text{ or } H_2O + CO_2).$$

Analogous reactions involving the hydroxides and bicarbonates of the other meteoric metals were also expected to occur, so that the metal chlorides would be an important reservoir for chlorine. Indeed, Murad *et al.* (1981) suggested that the release of large quantities of metals (about 10^3 kg) into the upper stratosphere would reduce for several years the harmful effects of chlorine released from chlorofluorocarbons.

Rodriquez *et al.* (1986), following the laboratory experiments demonstrating that NaOH, NaO_2 and NaO all reacted at the collision number with HCl (table 1), also included the reaction

$$NaO_2 + HCl \rightarrow NaCl + HO_2$$

in this scheme. However, Silver *et al.* (1985) showed from laboratory measurements that NaCl photolyses readily in the stratosphere. This would therefore form a catalytic cycle for recycling HCl back to active chlorine (Rowland and Rogers 1982). Rodriguez *et al.* (1986) used a one-dimensional model to explore this chemistry, from which they concluded that the ClO concentration near 50 km could increase by up to a factor of two, corresponding to a decrease in the calculated O_3 abundance by as much as 15%.

Thus the meteoric metals may greatly magnify the impact of chlorine at the top of the stratospheric ozone layer.

Lamb and Benson (1986) showed in a modelling study that NaCl, once formed from the reactions of HCl with NaOH, NaO_2 and other Na species, will readily polymerize or co-polymerize with other metal oxides or chlorides throughout the stratosphere. This polymerization is retarded in the upper stratosphere because of the short lifetime of NaCl with respect to photolysis. However, below 35 km, where the major concentrations of stratospheric ozone occur, polymerization becomes the major loss of NaCl. This is because of the large rate coefficients caused by the long-range dipole–dipole forces between the monomers, and the increasing surface area of the polymers as they grow. Polymer growth will only be limited by eventual diffusion out of the stratosphere, from which Lamb and Benson (1986) estimated an upper size limit for $(NaCl)_m$ of $m \approx 10^4$. They pointed out that other meteoric metals (e.g. Mg) form much more strongly bonded chlorides and oxychlorides, leading to even higher polymerization rates than for Na. Overall, they considered that there may be a net loss of several per cent of atmospheric chlorine into these polymers, which would be significant. However, this theory contains many assumptions required to calculate the rates of polymerization of the metal chlorides and oxides. These rates should now be studied experimentally.

Very recently, Prather and Rodriguez (1988) considered the impact of meteoric debris on the formation of the Antarctic ozone 'hole'. They suggested that atmospheric circulation leads to an accumulation of meteoric metal compounds in the Antarctic stratosphere at the beginning of the austral spring. Since the metals all tend to form alkaline species, their incorporation into acid stratospheric aerosols will neutralize the aerosol acidity. Gas-phase nitric acid can then be more readily incorporated into the aerosol phase, where it presumably forms metal nitrates. Meanwhile, the removal of HNO_3 from photochemical participation in the gas-phase chemistry of the lower stratosphere will cause the partitioning of chlorine to shift from HCl to the active forms Cl and ClO, so that photochemical ozone loss due to Cl (and Br) increases substantially. This mechanism would be substantiated if a future observation demonstrated that stratospheric aerosols in the Antarctic springtime have large abundances of Mg and Fe nitrates, compared with the trace levels observed in aerosols at mid-latitudes (Junge *et al.* 1961, Rosen 1971). Meteoric particles may indeed act as the nucleation centres around which stratospheric aerosols grow (Turco *et al.* 1981). In particular, because of the high concentrations of these particles in late winter, they may play a direct role in the formation of polar stratospheric clouds (PSCs), which have been shown to be very active sites for heterogeneous chemistry related to ozone removal (Aikin and McPeters 1986).

4.5. *Summary*

Models of Na chemistry in the mesosphere have been placed on a much firmer foundation following laboratory kinetic studies during the 1980s. Most of the observed features of the atomic-Na layer can be reproduced in modelling calculations, although a number of crucial rate coefficients remain to be measured in order to remove most of the remaining ambiguities from the models. Models of metal chemistry in the stratosphere indicate that meteoric metals may interact with the chlorine-catalysed removal of stratospheric ozone in a number of potentially important ways.

5. Future directions

The earlier sections of this review have illustrated that the study of metal chemistry in the upper atmosphere has reached an exciting juncture. Lidar observations of the metal-atom layers and laboratory investigations of their atmospheric chemistries have both made great strides over the last decade, to the point where many of the features of the metal layers that have aroused curiosity for the last fifty years are becoming understood. However, the deployment of metal lidars on a more routine basis has revealed a number of new phenomena, perhaps the most remarkable being the SSLs (section 2.2).

One major direction for future work will be comparative studies of different metals. This field has opened up now that the lidar technique has been adapted to study the neutral-atomic layers of five metals: Na, K, Li, Ca and Fe. In contrast with the very good correlation between metal ions in the mesosphere and those elements in chondritic meteorites, the correlation between the neutral-metal abundances and those in meteorites presents a rather different picture. This is illustrated in figure 24, where the *summertime* abundances are plotted relative to Na. The correlation of the three alkalis is excellent, although a plot of wintertime abundances would be less satisfactory because of the enhancement of Na and Li over K. However, Ca and Fe clearly do not correlate at all with the alkalis, especially bearing in mind that figure 24 is a logarithmic plot. Two major questions emerge from such comparative studies. The first is the reason for the relative depletion of Ca and Fe relative to Na. In particular, the mesospheric Ca abundance is about 120 times smaller than predicted from relative meteoritic abundances (Granier *et al.* 1989a). Recent studies in the author's laboratory (Plane and Nien (1990) and unpublished work) indicate that pertinent reactions of Ca, such as $CaO + O$ and $Ca + O_2 + N_2$, proceed with rate coefficients similar to those of Na. While it is possible that reactions such as $CaO_2 + O$ are very much slower than their Na analogues, the atomic Ca profile in the mesosphere is very similar in shape and altitude to that of Na (section 2.2.4), implying that their neutral chemistries are alike.

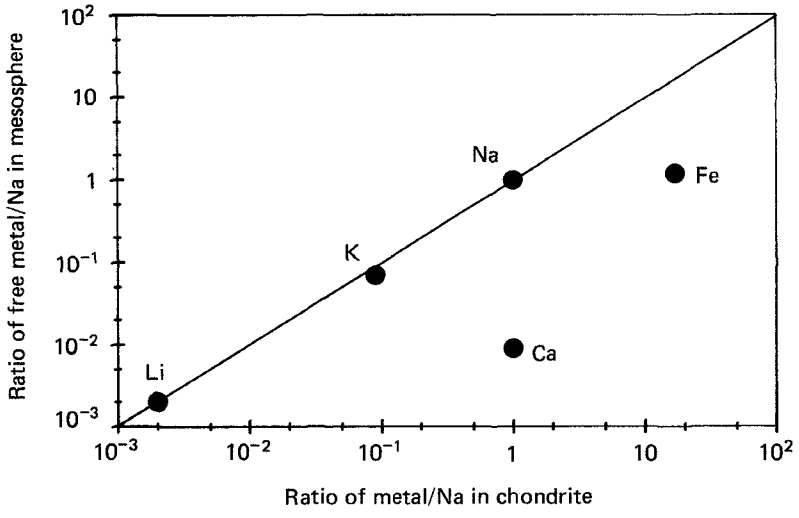

Figure 24. A comparison between the ratios of the column abundances of free metal atoms to sodium in the mesosphere, plotted against the ratio of the metals to sodium in chondritic meteorites. The mesospheric column abundances are for summertime. The data are plotted from Granier *et al.* (1989).

Furthermore, the Ca^+ ion abundance is even lower than that of Ca (Granier *et al.* 1985, 1989a), implying that ionization is not removing the bulk of ablated Ca. Indeed, one may be forced to conclude that the lower Ca abundance results from incomplete ablation of Ca from meteoroids (Granier 1989). No laboratory studies on the kinetics of pertinent Fe reactions appear to have been reported.

The second question is the different seasonal variations of the five metals. It has long been known that Na and Li are enhanced relative to K by a factor of about 5 in the wintertime at middle to high latitudes. Recent lidar work has demonstrated a small enhancement of Fe, and no apparent seasonal variation in Ca (section 2.2). A number of explanations have been advanced to account for the differences in the alkalis (section 4.1), starting with the theory of wintertime marine source (Donahue and Meier 1967). Hunten (1981) proposed that seasonal differences in ionization rates were responsible. Jegou *et al.* (1985) developed the theory of differences in the temperature dependences of the alkali ion cluster chemistry. Most recently, Swider (1985, 1987) and Plane (1989) postulated that the temperature dependences of the neutral chemistries of the alkali metals are sufficiently different to account for their seasonal differences. This last theory has received some support from a recent laboratory investigation of $NaO_2 + O$ (table 3). This is the first bimolecular Na reaction of atmospheric importance to have been studied that does not proceed at close to the collision number, implying that it has a reasonable activation energy ($> 10\,kJ\,mol^{-1}$). It is therefore quite conceivable that the analogous reactions of the three alkali superoxides have sufficiently different activation energies to cause significant seasonal differences in the degree of partitioning between the metal atoms and their superoxides, over the large seasonal temperature range in the high-latitude mesosphere. The seasonal variations in the peak heights of the layers, and the order of their peak heights ($Li > Na > K$), are all evidence that partitioning of the metals between atoms and superoxides is central to their mesospheric chemistry. Nevertheless, confirmation of this requires a demonstration in the laboratory that the reactions of the alkali superoxides with O atoms do indeed have sufficiently different activation energies.

Another difference in the chemistry of the alkali metals, which may contribute to their seasonal differences, is their formation of gas-phase tetroxide molecules. Ager and Howard (1986) first postulated the atmospheric formation of NaO_4, and Rajasekhar *et al.* (1989) found evidence for its formation in a laboratory study at 230 K. Rajasekhar *et al.* (1989) performed an *ab initio* optimization to determine the structure of the molecule, obtaining the O_4^- ion in the *cis* form, with the Na^+ ion completing a five-membered ring, as shown in figure 25. The alkali tetroxides have also been studied in inert-gas-matrix experiments, where the metal vapour and O_2 are co-condensed into the matrix. NaO_4 and KO_4 have been identified by infrared, Raman and ESR spectra (see references given by Rajasekhar *et al.* (1989)), but LiO_4 does not appear to be formed, presumably because of the small size of the Li^+ cation. Meanwhile, photolysis experiments on matrix-isolated tetroxides (Andrews 1976) showed that NaO_4 photolyses much more readily than NaO_2, whereas KO_4 has a relatively small photolysis cross-section above 200 nm. These differences need to be explored further.

Lidar observations of two or more metals *simultaneously* offer tremendous opportunities for understanding the chemistry. This is because a profile of the simultaneous relative abundances of the metals largely factors out the uncertainties contained in the meteoric-input function and the effects of turbulent transport, allowing differences in the chemistry to be highlighted instead. Granier *et al.* (1989b) have, for example, recently published the first simultaneous profiles of Fe and Na. Also,

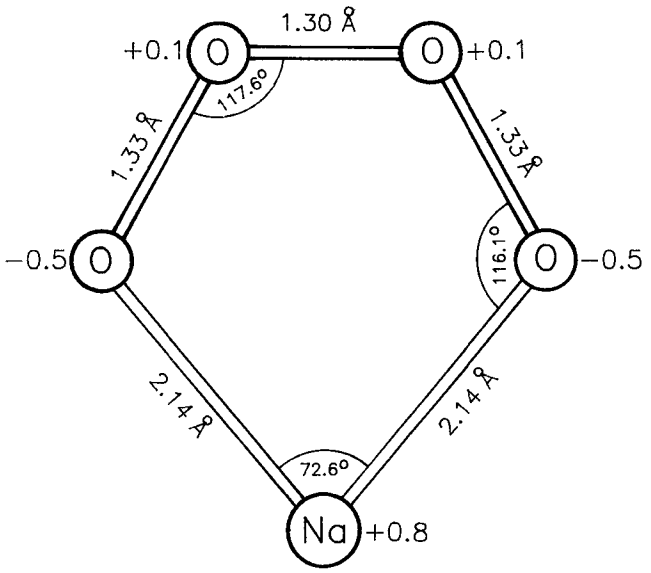

Figure 25. The optimized geometry (HF/6-31G*) of ground-state NaO_4 ($^2A_2$). The Mulliken electron populations are indicated as a signed number adjacent to each atomic centre. (Reproduced from Rajasekhar *et al.* (1989).)

the abundance of atomic Mg in the mesosphere would be of great interest. Laboratory experiments (C. Vinckier, Katholieke Universiteit Leuven, personal communication) indicate that the recombination reaction between Mg and O_2 is very slow, so that this metal may have a substantially different chemistry from the alkalis and Ca. Measurements on Mg will have to be made from space-based platforms because its resonance line at 285·2 nm ($Mg(3^1P_1)$–$Mg(3^1S)$) is absorbed by ozone in the lower atmosphere.

Two outstanding challenges for mesospheric models of Na are to explain the formation of SSLs (section 2.2.1) and to account for the extremely small scale-heights on the underside of the Na layer and the severe depletions in Na abundance that are observed in the summer at high latitudes (Gardner *et al.* 1988, Tilgner and von Zahn 1988). In both cases, the role of heterogeneous chemistry on both meteoric-dust particles and the ice crystals comprising noctilucent clouds has been postulated (Gardner *et al.* 1988, von Zahn and Hansen 1988, Beatty *et al.* 1989). Laboratory investigations into such heterogeneous effects, including the formation of large Na clusters and their interaction with electrons, are required. In addition, more complete observational data on SSLs are needed to confirm the apparent variations in their frequency of occurrence with latitude and time of day. More simultaneous measurements of SSLs by metal lidars and incoherent-scatter radars (Beatty *et al.* 1989) should confirm the link between their appearance and that of sporadic E.

Finally, the branching ratio of reaction (2) ($NaO+O \rightarrow Na(^2P, ^2S)+O_2$) still remains to be measured, fifty years after Chapman (1939) first postulated that it was responsible for the D-line emission at 589 nm in the nightglow. Current interest in the D-line emission derives from a proposal to make ground-based measurements of mesospheric O_3 (Llewellyn and Gardner 1989). The proposed method requires simultaneous lidar measurements of atomic Na and photometric measurements of the D-line nightglow intensity. The total nightglow emission is then given by expression

(4.3), from which $[O_3]$ can be calculated. This procedure will enable the *night-time* mesospheric O_3 density to be measured. By contrast, mesospheric O_3 is currently measured by the *dayglow* emission at 1·27 μm from $O_2(^1\Delta_g)$, either from rocket-borne *in situ* spectrometers (Evans *et al.* 1968) or from the Solar Mesospheric Explorer satellite (Barth *et al.* 1983). In addition, the proposed ground-based measurements can be used to ground-truth satellite observations, without requiring expensive rocketry. However, the branching ratio of reaction (2) is required in order to make the absolute measurements of mesospheric O_3. The determination of this branching ratio therefore has a high priority, although it is a challenging laboratory experiment.

In conclusion, the complementary developments in lidar technology and in laboratory kinetics techniques have yielded many important discoveries in the last few years. Much progress has been made in understanding the unusual aspects of metal behaviour in the upper atmosphere. Meanwhile, a number of remarkable new observations have been made, such as sporadic Na layers, and the surprising relative abundances of the free metal atoms. Laboratory studies have demonstrated the atmospheric importance of the metal superoxides, and perhaps the higher oxides such as the ozonides and tetroxides. Very little is known about the reactivities of these species, or the more stable species such as the carbonates and bicarbonates. Studies of the gas-phase chemistries of the more abundant metals like Fe and Mg are almost non-existent. However, these will be required as more lidar observations of Fe are made, and Mg may be observed from a future space-based platform. This review has also outlined the ancillary reasons for studying these metals, including their use as tracers of dynamics in the mesosphere, and for measuring the mesospheric ozone abundance. In addition, they have a complex and possibly important interaction with the chemistry of stratospheric ozone. This is certainly a field with a host of diverse and challenging questions for the future.

Acknowledgment

Support from the National Science Foundation, under Grant ATM-8820225, is gratefully acknowledged.

References

AGER, J. W., 1986, *Kinetics and diffusion of gas phase sodium species.* Ph.D. thesis, University of Colorado.

AGER, J. W., and HOWARD, C. J., 1986, *Geophys. Res. Lett.*, **13,** 1395; 1987, *J. chem. Phys.*, **87,** 921.

AGER, J. W., TALCOTT, C. L., and HOWARD, C. J., 1986, *J. chem. Phys.*, **85,** 5584.

AIKEN, A. C., and GOLDBERG, R. A., 1973, *J. geophys. Res.*, **78,** 734.

AIKEN, A. C., and MCPETERS, R. D., 1986, *Geophys. Res. Lett.*, **13,** 1300.

ANDREWS, L., 1976, *Molec. Spectrosc.*, **61,** 337.

ARNOLD, R., BOEHRINGER, H., and HENSCHEN, G., 1978, *Geophys. Res. Lett.*, **5,** 653.

ARNOLD, R., KRANKOWSKY, D., and MARIEN, K. H., 1977, *Nature, Lond.*, **267,** 30.

BARTH, C. A., RUSCH, D. W., THOMAS, R. J., MOUNT, G. H., ROTTMAN, G. J., THOMAS, G. E., SANDERS, R. W., and LAWRENCE, G. M., 1983, *Geophys. Res. Lett.*, **10,** 237.

BATES, D. R., 1947, *Terr. Magn. atmos. Elec.*, **52,** 71; 1954, *The Earth as a Planet*, edited by G. P. Kuiper (University of Chicago Press), Chap. 12; 1960, *Physics of the Upper Atmosphere*, edited by J. A. Ratcliffe (New York: Academic), Chap. 5.

BATES, D. R., and OJHA, P. C., 1980, *Nature, Lond.*, **286,** 790.

BATISTA, P. P., CLEMESHA, B. R., BATISTA, I. S., and SIMONICH, D. M., 1989, *J. geophys. Res.*, **94,** 1989.

BATISTA, P. P., CLEMESHA, B. R., SIMONICH, D. M., and KIRCHHOFF, V. M. J. H., 1985, *J. geophys. Res.*, **90,** 3881.

BEATTY, T. J., BILLS, R. E., KWON, K. H., and GARDNER, C. S., 1988, *Geophys. Res. Lett.*, **15,** 1137.
BEATTY, T. J., COLLINS, R. L., GARDNER, C. S., HOSTETLER, C. A., SECHRIST, C. F., and TEPLEY, C. A., 1989, *Geophys. Res. Lett.*, **16,** 1019.
BERNARD, R., 1938a, *Z. Phys.*, **110,** 291; 1938b, *C. r. hebd. Séanc. Acad. Sci., Paris*, **206,** 928.
BLAMONT, J. E., and DOHAHUE, T. M., 1964, *J. geophys. Res.*, **69,** 4093.
BLAMONT, J. E., DOHAHUE, T. M., and STULL, V. R., 1958, *Ann. Geophys.*, **14,** 253.
BOWMAN, M. R., GIBSON, A. J., and SANDFORD, M. C. W., 1969, *Nature, Lond.*, **221,** 456.
BRASSEUR, G., and SOLOMON, S., 1986, *Aeronomy of the Middle Atmosphere: Chemistry and Physics of the Stratosphere and the Mesosphere*, second edition (Boston: Reidel).
BROADFOOT, A. L., and JOHANSON, A. E., 1976, *J. geophys. Res.*, **81,** 1331.
BROWN, T. L., 1973, *Chem. Rev.*, **73,** 645.
BURNETT, C. R., LAMMER, W. E., NOVAK, W. T., and SIDES, V. T., 1972, *J. geophys. Res.*, **77,** 2934.
CABANNES, J., DUFAY, J., and GAUZIT, J., 1938, *C.r. hebd. Séanc. Acad. Sci., Paris*, **206,** 870.
CADLE, R. D., 1972, *EOS*, **53,** 812.
CADLE, R. D., and GRAMS, G. W., 1975, *Rev. Geophys. Space Phys.*, **13,** 475.
CARABETTA, R., and KASKAN, W. E., 1968, *J. phys. Chem.*, **72,** 2483.
CHAPMAN, S., 1939, *Astrophys. J.*, **30,** 151.
CHIMONAS, G., and AXFORD, W. I., 1968, *J. geophys. Res.*, **73,** 111.
CHARLSON, R. J., COVERT, D. S., LARSON, T. V., and WAGGONER, A. P., 1978, *Atmos. Environ.*, **12,** 39.
CIRA, 1972, *COSPAR International Reference Atmosphere* (Berlin: Akademie).
CLEMESHA, B. R., SIMONICH, D. M., BATISTA, P. P., and KIRCHHOFF, V. W. J. H., 1982, *J. geophys. Res.*, **87,** 181.
CLEMESHA, B. R., and SIMONICH, D. M., 1989, *J. atmos. terr. Phys.*, **51,** 145.
CLEMESHA, B. R., SIMONICH, D. M., BATISTA, P. P., and KIRCHHOFF, V. W. J. H., 1982, *J. geophys. Res.*, **87,** 181.
DAVIDOVITS, P., 1979, *Alkali Halide Vapours*, edited by P. Davidovits and D. L. McFadden (New York: Academic), p. 331.
DEJARDIN, G., 1938, *C.r. hebd. Séanc. Acad. Sci., Paris*, **206,** 930.
DELANEY, A. C., SHEDLOVSKY, J. P., and POLLOCK, W. H., 1974, *J. geophys. Res.*, **79,** 5646.
DELANNOY, J., and WEILL, G., 1958, *C.r. hebd. Séanc. Acad. Sci., Paris*, **246,** 2925.
DEMORE, W. B., MARGITAN, J. J., MOLINA, M. J., WATSON, R. T., GOLDEN, D. M., HAMPSON, R. F., KURYLO, M. J., HOWARD, C. J., and RAVISHARNKARA, A. R., 1985, *Chemical Kinetics and Photochemical Data for Use in Stratospheric Modeling* (Pasadena, California: JPL/NASA Publication 85-37).
DONAHUE, T. M., 1966, *International Dictionary of Geophysics*, edited by S. K. Runcorn (London: Pergamon Press).
DONAHUE, T. M., and BLAMONT, J. E., 1961, *Ann. Geophys.*, **17,** 116.
DONAHUE, T. M., and MEIER, R. R., 1967, *J. geophys. Res.*, **72,** 2803.
EVANS, W. F. J., HUNTEN, D. M., LLEWLLYN, E. J., and VALLANCE-JONES, A., 1968, *J. geophys. Res.*, **73,** 2885.
FELIX, F., KEENLISIDE, W., KENT, G., and SANDFORD, M. C., 1973, *Nature, Lond.*, **246,** 345.
FERGUSON, E. E., 1972, *Radio Sci.*, **7,** 397; 1978, *Geophys. Res. Lett.*, **5,** 1035.
FERGUSON, E. E., and FEHSENFELD, F. C., 1968, *J. geophys. Res.*, **73,** 6215.
FIOCCO, G., GRAMS, G., and VISCONTI, G., 1975, *J. atmos. terr. Phys.*, **37,** 1327.
FONTIJN, A., FELDER, W., and HOUGHTON, J. J., 1977, *Proceedings of 16th International Symposium on Combustion* (Pittsburgh: Combustion Institute), p. 871.
GADSDEN, M., 1964, *Ann. Geophys.*, **20,** 261; 1968, *J. atmos. terr. Phys.*, **30,** 151; 1969, *Ann Geophys.*, **25,** 667 and 721; 1970, *Ibid.*, **26,** 141; 1971, *Ibid.*, **27,** 401; 1983, *Proceedings of the Royal Meteorological Society Specialist Group in Atmosphere Chemistry* (Hertford College, Oxford).
GADSDEN, M., and SALMON, K., 1958, *Nature*, **182,** 1598.
GARDNER, C. S., and VOELZ, D. G., 1987, *J. geophys. Res.*, **92,** 4673.
GARDNER, C. S., SENFT, D. C., and KWON, K. H., 1988, *Nature, Lond.*, **332,** 142.
GARDNER, C. S., VOELZ, D. G., PHILBRICK, C. R., and SIPLER, D. P., 1986a, *J. Geophys. Res.*, **91,** 12131.
GARDNER, C. S., VOELZ, D. G., SECHRIST, C. F., and SEGAL, A. C., 1986b, *J. Geophys. Res.*, **91,** 13659.

GAULT, W. A., and RUNDLE, H. N., 1969, *Can. J. Phys.*, **47**, 85.
GERSH, M. E., SILVER, J. A., ZAHNISER, M. S., KOLB, C. E., BROWN, R. G., GOZEWSKI, C. M., KALLELIS, S., and WORMHOUDT, J. C., 1981, *Rev. scient. Instrum.*, **52**, 1213.
GIBSON, A. J., THOMAS, L., and BHATTACHACHARYYA, S. K., 1979, *Nature*, **281**, 131.
GOLDBERG, R. A., and AIKIN, A. C., 1973, *Science*, **180**, 296.
GRANIER, C., 1989, *Proceedings of the American Geophysical Union, San Francisco*, Paper SA32A-05.
GRANIER, C., JEGOU, J. P., and MEGIE, G., 1985, *Geophys. Res. Lett.*, **12**, 655; 1989a, *J. geophys. Res.*, **94**, 9917; 1989b, *Geophys. Res. Lett.*, **16**, 243.
GRANIER, C., and MEGIE, G., 1982, *Planet. Space Sci.*, **30**, 169.
GREER, R. G. H., and BEST, G., 1967, *Planet. Space Sci.*, **15**, 1857.
HAKE, R. D., ARNOLD, D. E., JACKSON, D. W., EVANS, W. E., FICKLIN, B. P., and LONG, R. A., 1972, *J. geophys. Res.*, **77**, 6839.
HANSON, W. B., and DONALDSON, J. S., 1967, *J. geophys. Res.*, **72**, 5513.
HENRIKSEN, K., DEEHR, C. S., SIVJEE, G. G., and MYRABO, H. K., 1986, *J. atmos. terr. Phys.*, **48**, 159.
HENRIKSEN, K., SIVJEE, G. G., and DEEHR, C. S., 1980, *J. geophys. Res.*, **85**, 5153.
HERMANN, U., EBERHARDT, P., HIDALGO, M. A., KOPP, E., and SMITH, L. G., 1978, *Space Research XVIII*, edited by M. J. Rycroft (Oxford: Pergamon), p. 245.
HERSCHBACH, D. R., 1966, *Adv. chem. Phys.*, **10**, 319.
HUGHES, D. W., 1978, *Cosmic Dust*, edited by J. A. M. McDonnell (Wiley: New York), chap. 3.
HUNTEN, D. M., 1954, *J. atmos. terr. Phys.*, **5**, 44; 1956, *The Radiating Atmosphere*, edited by B. M. McCormac (Dordrecht: Reidel), p. 3; 1967, *Space Sci. Rev.*, **6**, 1967; 1981, *Geophys. Res. Lett.*, **8**, 369.
HUNTEN, D. M., TURCO, R. P., and TOON, O. B., 1980, *J. atmos. Sci.*, **37**, 1342.
HUNTEN, D. M., and WALLACE, L., 1967, *J. geophys. Res.*, **72**, 69.
HUSAIN, D., 1989, *J. chem. Soc. Faraday Trans. 2*, **85**, 85.
HUSAIN, D., LEE, Y. H., and MARSHALL, P., 1987, *Combust. Flame*, **68**, 143.
HUSAIN, D., and MARSHALL, P., 1985, *Combust. Flame*, **60**, 81.
HUSAIN, D., MARSHALL, P., and PLANE, J. M. C., 1985a, *J. chem. Soc. Faraday Trans. 2*, **81**, 301; 1985b, *J. chem. Soc. Chem. Commun*, 1216; 1986, *J. Photochem.*, **32**, 1.
HUSAIN, D., and PLANE, J. M. C., 1982a, *J. chem. Soc. Faraday Trans. 2*, **78**, 163; 1982b, *Ibid.*, **78**, 1175.
HUSAIN, D., Plane, J. M. C., and CHEN CONG XIANG, 1984, *J. chem. Soc. Faraday Trans. 2*, **80**, 1619.
JEGOU, J.-P., CHANIN, M.-L., MEGIE, G., and BLAMONT, J. E., 1980, *Geophys. Res. Lett.*, **7**, 995.
JEGOU, J. P., GRANIER, C., CHANIN, M. L., and MEGIE, G., 1985, *Ann. Geophys.*, **3**, 163 and 299.
JENSEN, D. E., and JONES, G. A., 1982, *J. chem. Soc. Faraday Trans. 1*, **78**, 2842.
JUNGE, C. E., and MANSON, J. E., 1961, *J. geophys. Res.*, **66**, 2163.
JUNGE, C. E., CHAGNON, C. W., and MANSON, J. E., 1961, *J. Meteorol.*, **18**, 81.
JUNGE, C. E., OLDENBERG, O., and WASSON, J. T., 1962, *J. Geophys. Res.*, **67**, 1027.
KASKAN, W. E., 1965, *Proceedings of Tenth International Symposium on Combustion* (Pittsburgh: Combustion Institute), p. 41.
KAUFMAN, F., 1964, *Ann Geophys.*, **20**, 106.
KIRCHHOFF, V. W. J. H., CLEMESHA, B. R., and SIMONICH, D. M., 1979, *J. geophys. Res.*, **84**, 1323; 1981, *Ibid.*, **86**, 6892.
KIRCHHOFF, V. W. J. H., and TAKAHASHI, H., 1984, *Planet. Space Sci.*, **32**, 831.
KOLB, C. E., and ELGIN, J. R., 1976, *Nature, Lond.*, **263**, 488.
KOPP, E., and HERRMANN, U., 1984, *Ann. Geophys.*, **2**, 83.
KVIFTE, G., 1973, *Physics and Chemistry of Upper Atmospheres*, edited by B. M. McCormac (Dordrecht: Reidel), p. 158.
KWON, K. H., GARDNER, C. S., SENFT, D. C., ROESLER, F. L., and HARLANDER, J., 1987, *J. geophys. Res.*, **92**, 8781.
KWON, K. H., SENFT, D. C., and GARDNER, C. S., 1988, *J. geophys. Res.*, **93**, 14199.
LAMB, J. J., and BENSON, S. W., 1986, *J. geophys. Res.*, **91**, 8683.
LAZRUS, A. L., and GRANDRUD, B., 1971, *J. geophys. Res.*, **79**, 3424.
LEU, M. T., BIONDI, M. A., and JOHNSEN, R., 1973, *Phys. Rev.* A, **7**, 292.

LIU, S. C., and REID, G. C., 1979, *Geophys. Res. Lett.*, **6,** 283.
LLEWELLYN, E. J., and GARDNER, C. S., 1989, *Trans. Am. geophys. Union*, **70,** 1234.
LYTLE, E. A., and HUNTEN, D. M., 1959, *J. atmos. terr. Phys.*, **16,** 236.
MCEWAN, M. J., and PHILLIPS, L. F., 1975, *Chemistry of the Atmosphere* (London: Edward Arnold).
MCNUTT, D. P., and MACK, J. E., 1963, *J. geophys. Res.*, **68,** 3419.
MCSWEEN, H. Y., 1987, *Meteorites and their Parent Planets* (Cambridge University Press).
MASON, B., 1971, *Handbook of Elemental Abundances in Meteorites* (New York: Gordon and Breach).
MATHEWS, J. D., 1981, *J. atmos. terr. Phys.*, **43,** 549.
MEGIE, G., and BLAMONT, J. E., 1977, *Planet. Space Sci.*, **25,** 1093.
MEGIE, G., BOS, F., BLAMONT, J. E., and CHANIN, M. L., 1978, *Planet. Space Sci.*, **26,** 27.
MITCHELL, A. C. G., and ZEMANSKY, M. W., 1961, *Resonance Radiation and Excited Atoms*, 3rd edition (Cambridge University Press).
MURAD, E., SWIDER, W., and BENSON, S. W., 1981, *Nature, Lond.*, **289,** 273.
NARCISI, R. S., 1966, *Ann Geophys.*, **22,** 224; 1973, *Physics and Chemistry of Upper Atmospheres*, edited by B. M. McCormac (Dordrecht: Reidel), p. 173.
NEO, Y. P., and SHEPHERD, G. G., 1964, *Can. J. Phys.*, **42,** 1325.
NEUBER, R., VON DER GATHEN, P., and VON ZAHN, U., 1988, *J. Geophys. Res.*, **93,** 11093.
NEWMAN, A. L., 1988, *J. geophys. Res.*, **93,** 4067.
OMHOLT, A., 1957, *J. geophys. Res.*, **20,** 106.
PARUNGO, F., ACKERMAN, E., CALDWELL, W., and WEICKMANN, H. K., 1979, *Tellus*, **13,** 521.
PENKETT, S. A., ATKINS, D. H., and UNSWORTH, M. H., 1979, *Tellus*, **31,** 295.
PHILBRICK, C. R., BARNETT, J., GERNDT, R., OFFERMANN, D., PENDLETON, W. R., SCHLYTER, P., SCHMIDLIN, J. F., and WITT, G., 1984, *Adv. Space Res.*, **4,** 153.
PLANE, J. M. C., 1984, Kinetic studies of ground state alkali atoms. Ph.D. thesis, University of Cambridge; 1987, *J. phys. Chem.*, **91,** 6552; 1989, The seasonal chemistry of the alkali metals in the mesosphere. *Proceedings of the International Association of Geomagnetism and Aeronomy sixth Scientific Assembly, Exeter, U.K.*
PLANE, J. M. C., and HUSAIN, D., 1986, *J. chem. Soc. Faraday Trans. 2*, **82,** 2047.
PLANE, J. M. C., and NIEN, C.-F., 1990, *J. phys. Chem.*, **94,** 5255.
PLANE, J. M. C., and RAJASEKHAR, B., 1988a, *J. chem. Soc. Faraday Trans. 2*, **84,** 273; 1988b, *J. phys. Chem.*, **92,** 3884; 1989, *Ibid.*, **93,** 3135.
PLANE, J. M. C., RAJASEKHAR, B., and BARTOLOTTI, L., 1989a, *J. phys. Chem.*, **93,** 3141; 1990, *J. phys. Chem.*, **94,** 4161.
PRATHER, M. J., and RODRIGUEZ, J. M., 1988, *Geophys. Res. Lett.*, **15,** 1.
RAJASEKHAR, B., PLANE, J. M. C., and BARTOLOTTI, L., 1989, *J. phys. Chem.*, **93,** 7399.
RICHTER, E. S., and SECHRIST, C. F., 1979, *J. atmos. terr. Phys.*, **41,** 579.
RODRIGUEZ, J. M., KO, M. K. W., and SZE, N. D., 1986, *Geophys. Res. Lett.*, **13,** 499.
ROSEN, J. M., 1971, *J. appl. Meteorol.*, **10,** 1044.
ROWLAND, F. S., and MAKIDE, Y., 1982, *Geophys. Res. Lett.*, **9,** 473.
ROWLAND, F. S., and ROGERS, P. J., 1982, *Proc. Natl Acad. Sci. U.S.A.*, **79,** 2737.
ROWLETT, J. R., GARDNER, C. S., RICHTER, E. S., and SECHRIST, C. F., 1978, *Geophys. Res. Lett.*, **5,** 683.
SANDFORD, M. C. W., and GIBSON, A. J., 1970, *J. atmos. terr. Phys.*, **32,** 1423.
SENFT, D. C., COLLINS, R. L., and GARDNER, C. S., 1989, *Geophys. Res. Lett.*, **16,** 715.
SHEDLOVSKY, J. P., and PAISLEY, S., 1966, *Tellus*, **18,** 499.
SHIMAZAKI, T., 1985, *Minor Constituents in the Middle Atmosphere* (Dordrecht: Reidel).
SILVER, J. A., and KOLB, C. E., 1986, *J. phys. Chem.*, **90,** 3263.
SILVER, J. A., STANTON, A. C., ZAHNISER, M. S., and KOLB, C. E., 1984a, *J. phys. Chem.*, **88,** 3123.
SILVER, J. A., WORSNOP, D. R., FREEDMAN, A., and KOLB, C. E., 1985, *J. chem. Phys.*, **84,** 4718.
SILVER, J. A., ZAHNISER, M. S., STANTON, A. C., and KOLB, C. E., 1984b, *Proceedings of 20th International Symposium on Combustion* (Pittsburgh: The Combustion Institute), p. 605.
SIMONICH, D. M., CLEMESHA, B. R., and KIRCHHOFF, V. W. J. H.,1979, *J. geophys. Res.*, **84,** 1543.
SLIPHER, V. M., 1929, *Publ. astron. Soc. Pacific*, **41,** 262.
SMITH, I. W. M., 1980, *Kinetics and Dynamics of Elementary Gas Reactions* (London: Butterworths).

SMITH, L. L., and STEIGER, W. R., 1968, *J. geophys. Res.*, **73,** 2531.
SRIDHARAN, U. C., DI GUISEPPE, T. G., MCFADDEN, D. L., and DAVIDOVITS, P., 1979, *J. chem. Phys.*, **70,** 5422.
SULLIVAN, H. M., and HUNTEN, D. M., 1964, *Can. J. Phys.*, **42,** 937.
SWIDER, W., 1985, *Geophys. Res. Lett.*, **12,** 589; 1986, *J. geophys. Res.*, **91,** 6742; 1987, *Ibid.*, **92,** 5621.
SZE, N. D., KO, M. K. W., SWIDER, W., and MURAD, E., 1982, *Geophys. Res. Lett.*, **9,** 1187.
TALCOTT, C. L., AGER, J. W., and HOWARD, C. J., 1986, *J. chem. Phys.*, **84,** 6161.
TEPLEY, C. A., MERIWETHER, J. W., WALKER, J. C. G., and MATHEWS, J. D., 1981, *J. geophys. Res.*, **86,** 4831.
THOMAS, L., 1980, *Phil. Trans. R. Soc. London* A, **296,** 243.
THOMAS, L., and BOWMAN, M. R., 1972, *J. atmos. terr. Phys.*, **34,** 1843.
THOMAS, L., GIBSON, A. J., and BHATTACHARYYA, S. K., 1976, *Nature, Lond.*, **263,** 115.
THOMAS, L., ISHERWOOD, M. C., and BOWMAN, M. R., 1983, *J. atmos. terr. Phys.*, **45,** 587.
THOMAS, R. J., 1974, *Planet. Space Sci.*, **22,** 175.
TILGNER, C., and VON ZAHN, U., 1988, *J. geophys. Res.*, **93,** 8439.
TROE, J., 1977, *J. chem. Phys.*, **66,** 4745 and 4758.
TURCO, R. P., TOON, O. B., HAMILL, P., and WHITTEN, R. C., 1981, *J. geophys. Res.*, **86,** 1113.
VOLZ, F. E., and GOODY, R. M., 1962, *J. atmos. Sci.*, **19,** 385.
VON ZAHN, U., and HANSEN, G., 1988, *J. atmos. terr. Phys.*, **50,** 93; 1989, *Ibid.*, **51,** 147.
VON ZAHN, U., VON DER GATHEN, P., and HANSEN, G., 1987, *Geophys. Res. Lett.*, **14,** 76.
WAYNE, R. P., 1985, *Chemistry of Atmospheres* (Oxford University Press).
WORSNOP, D. R., ZAHNISER, M. S., KOLB, C. E., SHI, X., and HERSCHBACH, D. R., 1989, *Trans. Am. geophys. Union*, **70,** 1244.
ZBINDEN, P. A., HILDAGO, M. A., EBERHARDT, P., and GEISS, J., 1975, *Planet. Space Sci.*, **23,** 1261.